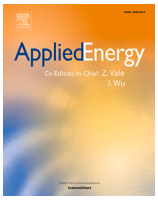
Applied Energy 426 (2026) 128765



Contents lists available at ScienceDirect

Applied Energy

journal homepage: www.elsevier.com/locate/apen



A multi-bound robust optimization approach for renewable-based VPP market participation considering intra-hourly uncertainty exposure

Hadi Nemati*, Álvaro Ortega, Enrique Lobato, Luis Rouco

Comillas Pontifical University, Institute for Research in Technology, Madrid, Spain

HIGHLIGHTS

- Novel multi-bound robust framework for RVPP bidding.
- Mitigates conservatism of classical robust optimization.
- Captures intra-hourly uncertainty, e.g., 15-minute market transitions.
- Distinguishes frequent deviations from extreme ones.
- Yields 24.9–49.2% normalized profit gains against the optimistic RO baseline.

ARTICLE INFO

Keywords:
Renewable-based virtual power plant
Multi-bound robust optimization
Intra-hourly uncertainty
Energy and reserve markets

ABSTRACT

With the ongoing transition of electricity markets worldwide from hourly to intra-hourly bidding, market participants—especially Renewable Energy Sources (RES)—gain improved opportunities to adjust energy and reserve schedules and to benefit from more accurate higher-resolution forecasts. However, this shift requires participants to update decision-making frameworks and to strengthen uncertainty management in order to fully exploit the new market potential. In particular, Renewable-Based Virtual Power Plants (RVPPs) aggregating dispatchable and non-dispatchable RES must account for these changes through market-oriented scheduling methods that efficiently address multiple uncertainties, including electricity prices, RES generation, and demand consumption. In this vein, this paper proposes a multi-bound robust optimization framework to simultaneously capture these uncertainties, explicitly incorporate intra-hourly variability, such as that arising under 15-minute market resolution, and differentiate the deviation levels (frequent, moderate deviations and rare, extreme ones) of uncertain parameters. The proposed approach yields less conservative and more implementable bidding and scheduling decisions, thus improving RVPP profitability in both energy and reserve markets. Simulation studies compare the proposed method with standard robust optimization and evaluate the operational, market-strategy, and economic impacts of quarter-hourly versus hourly market resolution. Results indicate that the normalized absolute differences, across different uncertainty-handling strategies, between hourly and 15-minute schedules are 18.0–34.2% for day-ahead traded energy, and 28.7–65.6% and 10.1–16.3% for upward and downward reserve traded in the secondary reserve market, respectively. Furthermore, using the optimistic single-bound robust optimization profit as a common normalization reference, the proposed multi-bound approach achieves normalized profit gains of 24.9–49.2% across the considered strategies.

1. Introduction

1.1. Motivation

Electricity markets worldwide are currently undergoing a fundamental structural transition toward higher temporal granularity, moving from traditional hourly settlements to sub-hourly (e.g., quarter-hourly) intervals. This shift is driven by evolving market rules aiming to harmonize market designs and, more critically, to facilitate the seamless integration of variable RES [1]. Within Europe, one recent example is the Spanish market's scheduled transition in October 2025, which will replace the standard 24 daily price points with 96 quarter-hourly intervals [2,3]. The primary goal of this transition is to align market schedules

* Corresponding author.
Email address: hnemati@comillas.edu (H. Nemati).

https://doi.org/10.1016/j.apenergy.2026.128765
Received 12 February 2026; Received in revised form 11 August 2026; Accepted 28 August 2026
Available online 3 September 2026
0306-2619/© 2026 The Authors. Published by Elsevier Ltd. This is an open access article under the CC BY-NC-ND license (http://creativecommons.org/licenses/by-nc-nd/4.0/).

Nomenclature

Abbreviations

C&CG	Column & Constraint Generation
CVaR	Conditional Value-at-Risk
D-RES	Dispatchable Renewable Energy Sources
DAM	Day-Ahead Market
DRO	Distributionally Robust Optimization
ESS	Energy Storage System
EV	Electric Vehicle
IGDT	Information Gap Decision Theory
MBRO	Multi-Bound Robust Optimization
MILP	Mixed Integer Linear Programming
ND-RES	Non-Dispatchable Renewable Energy Sources
PV	Photovoltaic
RES	Renewable Energy Sources
RO	Robust Optimization
RVPP	Renewable-Based Virtual Power Plant
SO	Stochastic Optimization
SRM	Secondary Reserve Market
VPP	Virtual Power Plant

Indices and Sets

$t \in \mathcal{T}$	Set of time periods
$u \in \mathcal{U}$	Set of Renewable-Based Virtual Power Plant (RVPP) units, comprising Non-Dispatchable RESs (ND-RESs) ($r \in \mathcal{R}$), Energy Storage Systems (ESSs) ($s \in \mathcal{S}$), Dispatchable RESs (D-RESs) ($c \in \mathcal{C}$), and demands ($d \in \mathcal{D}$)
$k \in \mathcal{K}$	Set of uncertainty bounds in Multi-Bound Robust Optimization (MBRO) approach
$t \in \mathcal{T}_k$	Set of worst-case time periods for bound k
$\Xi^{F/S}$	Sets of first- and second-level decision variables of the RVPP operator

Parameters

C_u	Marginal operation cost of unit u [€/MWh]
E_u	Rated energy capacity of unit u [MWh]
P_u	Rated power capacity or power forecast of unit u [MW]
R_u	Ramp rate of unit u [MW/min]
T^{SR}	Secondary reserve activation time [min]
β_u	Reserve provision limit factor of unit u [%]
Γ_k	Uncertainty budget for bound k [–]
Δt	Time step duration [h]
η_u	Efficiency of unit u [%]
λ_t	Forecast electricity market price during period t [€/MW, €/MWh]

Variables

$e_{u,t}$	Stored energy level of unit u at the end of period t [MWh]
p_t^{DA}	Power traded by the RVPP in the DAM during period t [MW]
$p_{u,t}$	Power dispatch of unit u during period t [MW]
r_t^{SR}	Reserve capacity traded by the RVPP in the Secondary Reserve Market (SRM) during period t [MW]
$r_{u,t}$	Reserve contribution provided by unit u during period t [MW]
σ_u	Fraction of unit u capacity allocated for reserve [%]
$y_{k,t}$	Auxiliary variable for uncertainty bound k during period t [MW, MWh]
$z_{k,t}$	Auxiliary variable for uncertainty budget of bound k during period t [–]
ϕ_k	Dual variable associated with the uncertain parameters of bound k [€, MW]
ζ_t	Dual variable associated with uncertain parameters during period t [€, MW]
$v_{u,t}$	Binary commitment status of unit u during period t [–]
$\chi_{u,k,t}$	Binary indicator for worst-case realization of unit u under bound k during period t [–]

Superscripts and Accents

A^{DA}	Related to the Day-Ahead Market (DAM)
A^{SR}	Related to the SRM
$A^{\uparrow}, A^{\downarrow}$	Upward and downward reserve directions
A^{+}, A^{-}	Charging and discharging states of ESSs
$\tilde{A}$	Median forecast value of an uncertain parameter
A^{*}	Optimal value of a variable
$\hat{A}, \check{A}$	Positive and negative deviations of an uncertain parameter from the forecast
$\bar{A}, \underline{A}$	Upper and lower bounds (e.g., limits or forecast bounds) of a parameter

more closely with physical grid operations, thereby incentivizing participants to balance supply and demand in near real-time and reducing reliance on costly adjustment mechanisms.

Under this transformed regulatory framework, the core platform for energy trading, the DAM, evolves from the traditional 24-period structure to a higher resolution timeline divided into 96 quarter-hourly intervals, in which generation and demand agents submit bids for each 15-minute slot, after which the market operator establishes market-clearing prices that reflect the immediate volatility of the grid more accurately than hourly averages [4]. Parallel to energy trading, the SRM, particularly for automatic frequency restoration reserve, remains the critical mechanism for the system operator to restore system frequency and power exchanges to scheduled values [5]. However, the technical requirements for providing reserve capacity are now tightly synchronized with the quarter-hourly energy settlement periods.

A RVPP operates as a unified entity that aggregates diverse assets, ranging from stochastic ND-RES and controllable D-RES to ESS and flexible demand, to provide grid services and enhance profitability [6]. For market participants, particularly RVPPs, this transition brings both opportunity and challenge. The shift to finer time resolutions exposes RVPPs to “intra-hourly” dynamics previously smoothed out in hourly models. While market structures have evolved to accommodate RES variability, traditional optimization models often lag behind, relying on coarse uncertainty handling approaches that miss rapid fluctuations in RES production, demand, and DAM/SRM prices at a 15-minute scale [7]. Consequently, fully leveraging high-resolution markets requires updating RVPP bidding strategies [8]. Specifically, uncertainty handling frameworks must be refined beyond hourly assumptions, ensuring that the RVPP can manage and profit from the granular volatility inherent in this new market era.

The transition from hourly to 15-minute market resolution is not merely a change in the number of scheduling intervals. It also changes the uncertainty and operational exposure of market participants, since variations in renewable generation, demand consumption, and market prices that were previously averaged within hourly intervals can directly affect quarter-hourly energy and reserve schedules. This is particularly relevant for RVPPs, whose flexibility depends on short-term operational constraints such as ESS state-of-charge evolution, charging/discharging limits, ramping-related reserve provision, and upward/downward reserve capacity limits. Accordingly, a technical framework for sub-hourly bidding must jointly address uncertainty representation and unit-level feasibility at the quarter-hourly scale, rather than only increasing the number of time periods in an hourly model.

1.2. Literature review

The participation of Virtual Power Plants (VPPs) in the DAM has been extensively researched, particularly regarding the management of uncertainties associated with RES production and demand. Numerous studies employ Robust Optimization (RO) and Stochastic Optimization (SO) techniques to address these challenges [9–14]. For instance, Liu et al. [9] proposed a two-stage RO approach that incorporates a refined demand response strategy, solving the problem via the Column & Constraint Generation (C&CG) algorithm with fuzzy-based subproblems. Wu et al. [10] developed a two-stage Distributionally Robust Optimization (DRO) model for rural VPPs integrating biomass and RES, utilizing a dual vertices fixing algorithm to handle correlated wind and solar uncertainties. The integration of ESS was addressed by Feng et al. [11], who applied an improved nested C&CG algorithm within a two-stage DRO framework to manage power deviations. Beyond electricity, Li et al. [12] extended RO to multi-energy VPPs participating in both energy and peak-regulation markets. Falabretti et al. [13] utilized a Monte Carlo-based two-stage SO for RVPPs with Electric Vehicle (EV) charging stations, while Cao et al. [14] explored carbon trading flexibility using scenario-based DRO. However, a significant limitation of these works is the neglect of market price uncertainty, a factor that critically impacts VPP profitability.

To address this limitation, recent literature has incorporated market price uncertainty alongside generation variability [15–19]. Wang et al. [15] introduced a two-stage DRO model that handles DAM price uncertainty in the first stage and utilizes Conditional Value-at-Risk (CVaR) to manage real-time price risks. Incorporating risk preferences, Xiao et al. [17] proposed an SO framework capable of modeling both risk-seeking and risk-averse strategies, while Shafiekhani et al. [18] employed Information Gap Decision Theory (IGDT) to balance economic viability and emission minimization under different risk attitudes. Advanced bi-level structures have also been proposed; Afzali et al. [19] developed a risk-aware SO–RO strategy for energy and flexibility markets, reformulating the problem as a Mixed Integer Linear Programming (MILP) to ensure global optimality. Furthermore, hybrid uncertainty handling methods have emerged, such as the data-driven RO model by Ma et al. [20], which captures price uncertainty via data-driven techniques and physical uncertainties via RO. Others have extended these frameworks to price-maker VPPs [21] and low-carbon scheduling [22], simultaneously quantifying uncertainties in generation, load, and prices.

While the aforementioned studies focus primarily on energy trading, VPPs can also leverage flexible assets to provide ancillary services, enhancing system stability and their revenue [6,23–32]. Yang et al. [6] utilized non-linear programming for joint participation in energy, reserve, and regulation markets, characterizing uncertainties via confidence intervals. Shang et al. [23] applied an interval probability method to manage volatility across emergency levels in frequency modulation markets. Feng et al. [24] proposed a chance-constrained DRO framework defining interval ambiguity sets for RES generation. Du et al. [25] modeled the physical-economic feasible region of VPPs within a two-stage optimization for joint markets, and Siqin et al. [26] addressed simultaneous energy, reserve, and carbon trading. Additionally, Esfahani et al. [27] focused on frequency regulation from aggregated small ESS, employing an SO–RO approach with CVaR to manage capacity and price risks. Nokandi et al. [28] developed a three-stage SO model incorporating intraday demand response exchanges, while Zamani et al. [29] applied point estimate methods for joint electrical and thermal scheduling. Li et al. [33] introduce a risk-aware SO framework for multi-market bidding that broadens the scope of uncertainty to encompass not only RES variability but also the compliance willingness of users. Robust frameworks have also been refined; Nemati et al. proposed methods capturing asymmetric uncertainties in sequential markets [30], handling non-linear couplings in simultaneous markets via flexible RO [31], and integrating concentrated solar power through reformulated two-stage RO [32].

Although several robustness-based frameworks have been proposed to manage multiple uncertainty sources in VPP/RVPP scheduling, most of them reduce conservatism by adding recourse decisions, scenario-based descriptions, or distributional ambiguity sets. In contrast, the proposed MBRO framework reduces conservatism by enriching the uncertainty-set structure itself. Specifically, instead of representing each uncertain parameter with a single interval and a single uncertainty budget, the proposed approach uses multiple nested bounds with separate budgets. This allows frequent moderate deviations and rare extreme deviations to be modeled separately within a single-level MILP formulation. Therefore, the RVPP can obtain protection against severe uncertainty realizations without forcing all protected deviations to take their worst-case values, which leads to less conservative and more balanced bidding decisions in high-resolution energy and reserve markets.

As discussed above, the domain of hourly multi-market participation is quite mature, with sophisticated optimization techniques handling diverse uncertainties. However, the transition of electricity markets toward higher temporal resolution leaves existing hourly models insufficient for capturing intra-hourly dynamics. Limited research has focused on addressing this shift [34–36]. Li et al. [34] proposed a DRO strategy for a 96-period market, but they simplified market prices to hourly resolution to aid convergence. Yuanyuan et al. [35] focused on a 96-period declaration strategy with flexible ramping products, yet their uncertainty modeling was limited to wind power. Wang et al. [36] utilized Italian market data to model hourly DAM and 15-minute reserve markets but did not fully account for intra-hourly price and demand volatility. Consequently, there remains a critical gap for a holistic approach that enables VPP participation in high-resolution energy and reserve markets while comprehensively accounting for the intra-hourly exposure to uncertainties in market prices, RES generation, and demand. In this context, Table 1 contrasts the key features of this study against the reviewed literature.

To fill the identified gaps and align with the transition of electricity markets worldwide toward sub-hourly resolution, this paper proposes a novel bidding strategy for RVPP participation in the DAM and SRM. The core contribution is the development of an MBRO framework capable of simultaneously managing the multiple uncertainties inherent in electricity prices, ND-RES production, and demand. The concept of MBRO was developed in [37] to mitigate the inherent conservatism of classical RO theory [38]. The proposed MBRO framework in this paper fundamentally differs from the traditional RO approach by explicitly modeling intra-hourly uncertainty exposure. Standard RO formulations typically apply a single global robustness budget across the time horizon, often resulting in a binary outcome where specific time periods are fully protected against maximum possible deviations—leading to excessive conservatism—while remaining periods are treated optimistically with no protection once the budget is exhausted. In contrast, the proposed MBRO discretizes the uncertainty spectrum into distinct “bounds” corresponding to different deviation magnitudes. The RVPP operator can, in this way, define flexible robustness budgets for each bound rather than relying on a single global parameter. By assigning higher budgets to lower bounds (representing frequent, moderate deviations) and lower budgets to upper bounds (representing rare, extreme deviations), the formulation ensures broader protection across more time intervals without forcing the solution to accommodate the maximum protection for every period. The aim is to effectively balance risk and profitability to yield practical bidding decisions tailored to high-resolution markets. The study further details the mathematical proof for the linear reformulation of this bi-level MBRO problem and validates the approach through extensive comparisons with classic RO and hourly-resolution benchmarks.

Table 1
Comparison of the approach in this paper and recent literature.

	Market		Market resolution		Uncertainty			Intra-hourly	Uncertainty treatment		Method
Ref.	Energy	Reserve	24-period	96-period	Price	RES	Demand	uncertainty	Single-bound	Multi-bound	
[9]	•		•			•			•		RO
[10,11]	•		•			•			•		DRO
[12]	•		•			•	•		•		RO
[13]	•		•			•	•				SO
[14]	•		•			•	•		•		DRO
[15]	•		•		•				•		CVaR–DRO
[16,17]	•		•		•	•					SO
[18]	•		•		•	•			•		IGDT
[19]	•		•		•	•			•		SO–RO
[20,22]	•		•		•	•	•		•		RO
[21]	•		•		•	•	•		•		DRO
[6,23]	•	•	•			•					Probability distribution
[24]	•	•	•			•					Chance constrained DRO
[25]	•	•	•			•	•				Chance constrained
[26]	•	•	•		•	•					DRO
[27]	•	•	•		•		•		•		SO–RO
[28,29,33]	•	•	•		•	•	•				SO
[30–32]	•	•	•		•	•	•		•		RO
[34]	•			•		•			•		DRO
[35]	•	•		•		•			•		DRO
[36]	•	•		•		•			•		RO
This paper	•	•		•	•	•	•	•		•	MBRO

1.3. Paper contributions

The main contributions of this paper are outlined as follows:

- **Proposes an MBRO bidding framework for RVPP market participation:** This approach simultaneously handles multiple uncertainties related to electricity prices, ND-RES production, and demand consumption. Unlike classical RO, which often yields overly conservative solutions by treating all uncertainty realizations uniformly, the proposed MBRO formulation provides a more realistic representation of uncertainty. By distinguishing between frequent, moderate deviations and rare, extreme ones, the approach generates less conservative, more implementable schedules that enhance the profitability of the RVPP.
- **Addresses intra-hourly uncertainty exposure in market transitions:** The model aligns with the recent transition of electricity markets from hourly to finer temporal bidding structures. The study highlights that ignoring intra-hour uncertainty leads to a systematic misestimation of imbalance risks by smoothing out intra-hour volatility in RVPP trading and scheduling. This paper provides more realistic and granular bidding decisions for modern electricity markets by handling uncertainty at a quarter-hourly time resolution.
- **Quantifies the value of multi-bound robustness and granularity:** A rigorous comparative analysis with classic RO and Wasserstein-DRO benchmark models is conducted across different uncertainty-handling strategies. The analysis also examines market-resolution effects, budget sensitivity, out-of-sample implementability, and computational tractability, showing how MBRO balances robustness, profitability, and practical applicability in the new market era.

The remainder of this paper is organized as follows. Section 2 defines the operational scope and problem statement. The mathematical formulation of the proposed MBRO strategy for the RVPP's joint participation in the DAM and SRM is derived in Section 3. A comprehensive numerical analysis and discussion of the results are presented in Section 4. Finally, Section 5 summarizes the key findings and suggests potential directions for future research.

2. Problem description

The operational framework of the proposed RVPP is conceptually illustrated in Fig. 1. As depicted, the RVPP functions as a central aggregator that coordinates a diverse portfolio of assets, including D-RES (e.g., hydro plant), ND-RES (e.g., wind and solar Photovoltaic (PV)), demand, and ESS. The figure distinguishes between two primary interaction flows essential for the RVPP's operation. First, the electrical energy flow (blue lines) represents the physical power exchange between the power grid and the internal assets. The RVPP facilitates the grid integration of ND-RES by balancing their variability with controllable dispatchable units and storage, with the aim of ensuring technical feasibility and reliable demand satisfaction. Second, the data and decision flow (red dashed lines) represents the decision-making core where the RVPP operator gathers technical data and availability forecasts from internal units while simultaneously monitoring market conditions. Based on this information, the operator submits optimal bids to the DAM for energy trading and the SRM for ancillary services. In this framework, the RVPP is modeled as a price-taker and submits zero-price bids to ensure dispatch. The rationale for this assumption lies in the RVPP's relatively small size compared to the grid size, as well as the economic characteristics of its aggregated assets, which are primarily ND-RES with low marginal operating costs. Once the markets clear, the operator disaggregates the commitments, communicating specific dispatch set-points back to the internal units to maintain the schedule.

A critical challenge for the RVPP operator is managing the multiple uncertainties in units and prices highlighted in the optimization block of Fig. 1. To maximize profitability while ensuring robustness, the operator must account for stochasticity in ND-RES production, demand consumption, and market prices. While recent literature suggests that flexible RO allows operators to adjust conservatism via uncertainty budgets [20,22,30,36], standard RO approaches often treat all deviations uniformly. This can lead to overly conservative schedules that fail to capture the nuances of more granular bidding structures. To address these limitations, this study proposes an MBRO approach, mathematically formulated in the following section. Unlike classical methods, MBRO segments the uncertainty spectrum into distinct bounds (e.g., frequent small deviations vs. rare extreme events). This granular handling of uncertainty allows the RVPP to prioritize frequent deviations over rare sharp ones, resulting in less conservative bidding strategies

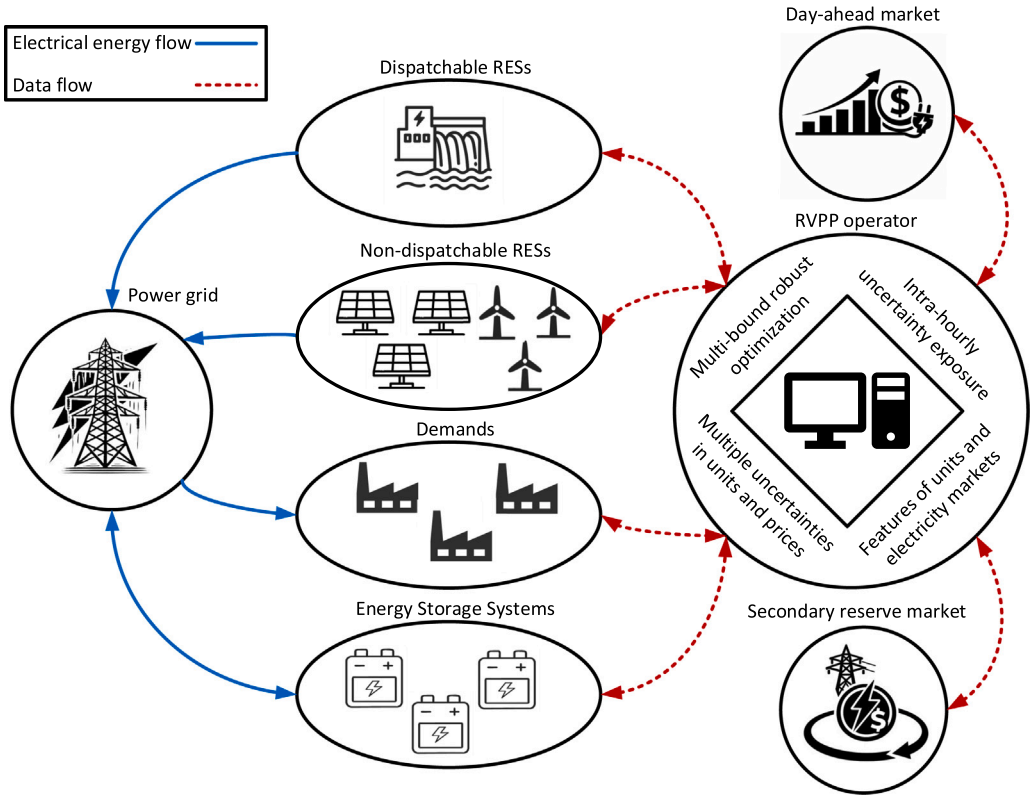


Fig. 1. The operational framework of the proposed RVPP.

that maintain computational efficiency and are better aligned with the high-resolution requirements of modern energy and reserve markets.

3. Formulation

This section details the mathematical framework of the proposed MBRO approach for the RVPP operation. Section 3.1 first outlines the deterministic model for participation in the DAM and SRM in line with existing literature [20,22,30,31,36]. Subsequently, to effectively address the inherent volatility of electricity prices, generation from ND-RES, and demand consumption, Section 3.2 introduces the proposed MBRO framework as a novel contribution of this work.

3.1. Deterministic problem

3.1.1. Objective function

The objective function defined in (1) serves to maximize the RVPP's total operational profit derived from participation in both the DAM and the SRM. This formulation aggregates revenues from energy trading and bidirectional reserve provision, subtracting the operational expenditures associated with D-RESs, ND-RESs, and ESSs.

$$\max_{\Xi^F} \sum_{t\in\mathcal{T}} \lambda_t^{DA} p_t^{DA} \Delta t + \sum_{t\in\mathcal{T}} \left[\lambda_t^{SR,\uparrow} r_t^{SR,\uparrow} + \lambda_t^{SR,\downarrow} r_t^{SR,\downarrow}\right] - \sum_{t\in\mathcal{T}}\sum_{c\in\mathscr{C}} C_c p_{c,t} \Delta t - \sum_{t\in\mathcal{T}}\sum_{r\in\mathcal{R}} C_r p_{r,t} \Delta t - \sum_{t\in\mathcal{T}}\sum_{s\in\mathcal{S}} C_s p_{s,t} \Delta t \tag{1}$$

3.1.2. Supply–demand constraints

The fundamental requirement for the RVPP to meet its market obligations is the preservation of power balance at every time step. The supply–demand constraint (2) is thus defined to ensure that the RVPP's aggregated output matches its commitment regardless of whether secondary reserves are activated in the upward or downward direction, or remain inactive. To implement this, the model employs the reserve state vectors, $\boldsymbol{r}_t^{SR} = \{r_t^{SR,\uparrow}, -r_t^{SR,\downarrow}, 0\}$ for the RVPP, and $\boldsymbol{r}_{u,t} = \{r_{u,t}^{\uparrow}, -r_{u,t}^{\downarrow}, 0\}$ for individual assets $u \in \mathscr{U}$, including ND-RESs, ESSs, D-RESs, and demands. Thus, Eq. (2) describes a system of three distinct balance equations that fully capture the deterministic response required for each activation scenario [31].

$$\sum_{r\in\mathcal{R}} \left[p_{r,t} + \boldsymbol{r}_{r,t}\right] + \sum_{s\in\mathcal{S}} \left[p_{s,t} + \boldsymbol{r}_{s,t}\right] + \sum_{c\in\mathscr{C}} \left[p_{c,t} + \boldsymbol{r}_{c,t}\right] - \sum_{d\in\mathscr{D}} \left[p_{d,t} - \boldsymbol{r}_{d,t}\right] = p_t^{DA} + \boldsymbol{r}_t^{SR}\ ; \qquad \forall t \in \mathcal{T} \tag{2}$$

3.1.3. Dispatchable unit constraints

In this study, D-RES units are defined as renewable energy assets that can be operated in a controllable manner, similar to conventional thermal units. These resources include units such as hydro plants and can be scheduled by the RVPP within their operational limits to provide both energy and reserve. To model this controllability, constraints (3a) and (3b) define the operational limits for energy and reserve provision, contingent on the binary commitment variable $v_{c,t}$. Constraint (3c) ensures compliance with daily energy production limits, often dictated by seasonal water management policies (e.g., for hydro plants). Finally, temporal constraints regarding minimum up and down times are omitted here for brevity but follow the standard MILP formulation presented in [39].

$$p_{c,t} + r_{c,t}^{\uparrow} \le \bar{P}_c v_{c,t}\ ; \qquad \forall c,t \in \mathscr{C},\mathcal{T} \tag{3a}$$

$$\underline{P}_c v_{c,t} \le p_{c,t} - r_{c,t}^{\downarrow}\ ; \qquad \forall c,t \in \mathscr{C},\mathcal{T} \tag{3b}$$

$$\sum_{t\in\mathcal{T}} \left[p_{c,t}\Delta t + r_{c,t}^{\uparrow}\Delta t\right] \le \bar{E}_c\ ; \qquad \forall c \in \mathscr{C} \tag{3c}$$

3.1.4. Non-dispatchable unit constraints

The category of ND-RES includes stochastic assets like wind and solar PV, where the maximum output is mostly determined by meteorological forecasts rather than operator dispatch. Despite this, they can participate in the SRM by modulating curtailment levels: downward reserve is provided by reducing output, whereas upward reserve is available when the unit is pre-curtailed below its available potential [40,41]. In the model, Constraint (4a) caps production at the forecasted limit $P_{r,t}$, while Constraint (4b) defines the lower feasibility bounds for simultaneous energy and reserve schedules.

$$p_{r,t} + r^{\uparrow}_{r,t} \le P_{r,t} \; ; \qquad \forall r, t \in \mathscr{R}, \mathscr{T} \qquad (4a)$$

$$\underline{P}_{r} \le p_{r,t} - r^{\downarrow}_{r,t} \; ; \qquad \forall r, t \in \mathscr{R}, \mathscr{T} \qquad (4b)$$

3.1.5. Demand constraints

Electrical demand represents a source of both flexibility and stochasticity within the RVPP portfolio [24]. The feasible operating domain, which accounts for simultaneous power consumption and reserve provision, is established by constraints (5a) and (5b), where the lower consumption limit is governed by forecast uncertainty. The minimum energy requirement over the scheduling horizon is enforced by constraint (5c).

$$P_{d,t} \le p_{d,t} - r^{\uparrow}_{d,t} \; ; \qquad \forall d, t \in \mathscr{D}, \mathscr{T} \qquad (5a)$$

$$p_{d,t} + r^{\downarrow}_{d,t} \le \bar{P}_{d} \; ; \qquad \forall d, t \in \mathscr{D}, \mathscr{T} \qquad (5b)$$

$$\underline{E}_{d} \le \sum_{t \in \mathscr{T}} \left[p_{d,t} \Delta t - r^{\uparrow}_{d,t} \Delta t \right] \; ; \qquad \forall d \in \mathscr{D} \qquad (5c)$$

3.1.6. ESS constraints

ESSs are rapidly gaining popularity as flexibility provision assets, due to their capability to efficiently mitigate the intermittency of ND-RESs, among other interesting features. The mathematical framework governing ESS operation is presented in (6), enabling simultaneous optimization of energy arbitrage and reserve provision [32]. Constraints (6a)–(6d) establish the operational boundaries for ESS power and reserve, ensuring that sufficient capacity is maintained for both upward and downward reserve provision in both charging (+) and discharging (−) states. The binary variable $v_{s,t}$ is utilized to explicitly differentiate between the charging and discharging states, thus preventing simultaneous operation. The resulting net power output and total reserve capacity are aggregated in (6e)–(6g). Regarding energy management, Eq. (6h) tracks the state of charge dynamics, while constraint (6i) imposes a daily cyclic balance by equating the initial and final stored energy. Note that this constraint can be relaxed according to RVPP operator needs. The allocation of storage capacity for upward and downward reserves is governed by coefficients $\sigma^{\uparrow}_{s}$ and $\sigma^{\downarrow}_{s}$ in (6j)–(6k). Finally, constraint (6l) adjusts the feasible energy limits to account for the energy allocated to reserve capacity.

$$\underline{P}^{+}_{s} v_{s,t} \le p^{+}_{s,t} - r^{+,\uparrow}_{s,t} \; ; \qquad \forall s, t \in \mathscr{S}, \mathscr{T} \qquad (6a)$$

$$p^{+}_{s,t} + r^{+,\downarrow}_{s,t} \le \bar{P}^{+}_{s} v_{s,t} \; ; \qquad \forall s, t \in \mathscr{S}, \mathscr{T} \qquad (6b)$$

$$p^{-}_{s,t} + r^{-,\uparrow}_{s,t} \le \bar{P}^{-}_{s} \left(1 - v_{s,t}\right) \; ; \qquad \forall s, t \in \mathscr{S}, \mathscr{T} \qquad (6c)$$

$$\underline{P}^{-}_{s} \left(1 - v_{s,t}\right) \le p^{-}_{s,t} - r^{-,\downarrow}_{s,t} \; ; \qquad \forall s, t \in \mathscr{S}, \mathscr{T} \qquad (6d)$$

$$p_{s,t} = p^{-}_{s,t} - p^{+}_{s,t} \; ; \qquad \forall s, t \in \mathscr{S}, \mathscr{T} \qquad (6e)$$

$$r^{\uparrow}_{s,t} = r^{+,\uparrow}_{s,t} + r^{-,\uparrow}_{s,t} \; ; \qquad \forall s, t \in \mathscr{S}, \mathscr{T} \qquad (6f)$$

$$r^{\downarrow}_{s,t} = r^{+,\downarrow}_{s,t} + r^{-,\downarrow}_{s,t} \; ; \qquad \forall s, t \in \mathscr{S}, \mathscr{T} \qquad (6g)$$

$$e_{s,t} = e_{s,t-1} + p^{+}_{s,t} \eta^{+}_{s} \Delta t - \frac{p^{-}_{s,t} \Delta t}{\eta^{-}_{s}} \; ; \qquad \forall s, t \in \mathscr{S}, \mathscr{T} \setminus \{1\} \qquad (6h)$$

$$e_{s,1} = e_{s,|\mathscr{T}|} \; ; \qquad \forall s \in \mathscr{S} \qquad (6i)$$

$$\sum_{t \in \mathscr{T}} \frac{r^{\uparrow}_{s,t} \Delta t}{\eta^{-}_{s}} \le \sigma^{\uparrow}_{s} \left(\bar{E}_{s} - \underline{E}_{s}\right) \; ; \qquad \forall s \in \mathscr{S} \qquad (6j)$$

$$\sum_{t \in \mathscr{T}} r^{\downarrow}_{s,t} \eta^{+}_{s} \Delta t \le \sigma^{\downarrow}_{s} \left(\bar{E}_{s} - \underline{E}_{s}\right) \; ; \qquad \forall s \in \mathscr{S} \qquad (6k)$$

$$\underline{E}_{s} + \sigma^{\uparrow}_{s} \left(\bar{E}_{s} - \underline{E}_{s}\right) \le e_{s,t} \le \bar{E}_{s} - \sigma^{\downarrow}_{s} \left(\bar{E}_{s} - \underline{E}_{s}\right) ; \qquad \forall s, t \in \mathscr{S}, \mathscr{T} \qquad (6l)$$

3.1.7. Reserve provision constraints

Although the energy production limits are technology-specific, the mathematical framework governing reserve provision is unified across the RVPP portfolio and is presented in (7). Constraints (7a) and (7b) determine the permissible upward and downward reserve capacity for each asset $u \in \mathscr{U}$ that comprises the RVPP portfolio. This reserve capacity is strictly bounded by their ramp-rate characteristics and the secondary reserve activation time. Constraints (7c) and (7d) cap the reserve contribution based on the unit's maximum electrical rating and the reserve provision limit factors assigned by the RVPP operator [31].

$$r^{\uparrow}_{u,t} \le T^{SR} R^{\uparrow}_{u} \; ; \qquad \forall u, t \in \mathscr{U}, \mathscr{T} \qquad (7a)$$

$$r^{\downarrow}_{u,t} \le T^{SR} R^{\downarrow}_{u} \; ; \qquad \forall u, t \in \mathscr{U}, \mathscr{T} \qquad (7b)$$

$$r^{\uparrow}_{u,t} \le \beta^{\uparrow}_{u} \bar{P}_{u} \; ; \qquad \forall u, t \in \mathscr{U}, \mathscr{T} \qquad (7c)$$

$$r^{\downarrow}_{u,t} \le \beta^{\downarrow}_{u} \bar{P}_{u} \; ; \qquad \forall u, t \in \mathscr{U}, \mathscr{T} \qquad (7d)$$

3.2. Multi-bound robust model

The deterministic formulation in Section 3.1 assumes perfect foresight, neglecting the inherent volatility of market prices and asset energy outputs. However, uncertainty in electricity and reserve prices, as well as variations in ND-RES generation and demand, can significantly impact the RVPP's financial performance. To mitigate these risks, the optimization problem is extended to an MBRO framework in Section 3.2.1. This is formulated as a bi-level problem: the first level maximizes the RVPP's objective function analogous to the deterministic model, while the second level minimizes the RVPP's profit by identifying the worst-case realization of uncertain parameters within defined bounds. Unlike traditional RO, which typically defines a single interval for uncertainty (often leading to overly conservative solutions dominated by extreme scenarios), the MBRO framework segments the uncertainty spectrum into distinct bounds (e.g., deviation levels). By assigning specific budgets to these separate bounds, the model captures a more granular profile of risk. To solve the resulting bi-level problem efficiently with standard optimization tools, the inner worst-case (second-level) problem is reformulated into an equivalent tractable form, enabling a single-level MILP implementation. Section 3.2.2 details this reformulation of the second-level uncertainty problem. Finally, Section 3.2.3 presents the final MILP formulation of the MBRO model as a single-level problem solvable by commercial MILP solvers.

3.2.1. Bi-level formulation

The bi-level MBRO problem for the RVPP's participation in the DAM and SRM is formulated in (8)–(9). The objective function (8) seeks to maximize the base deterministic profit (represented by the first two lines, which account for expected market revenues based on price forecasts and unit operational costs) while explicitly subtracting the worst-case revenue loss caused by electricity price uncertainty in the third line. The value of the worst-case protection functions in the third line of (8) is referred to as the *robust cost*. This quantity enters the objective function as a penalty and represents the worst-case revenue loss associated with market-price uncertainty under the adopted uncertainty budgets. Economically, it quantifies the amount of nominal expected objective value that the RVPP operator gives up at the bidding stage in order to hedge against adverse price realizations. The set

of first-level decision variables, Ξ^F, remains consistent with the deterministic model presented in Section 3.1. The worst-case realization of market prices is determined by the inner maximization problem, which is performed over the sets of worst-case time periods for DAM and SRM prices ($\mathcal{T}_k^{DA}, \mathcal{T}_k^{SR,\uparrow}, \mathcal{T}_k^{SR,\downarrow}$). The cardinality of these sets is equal to the value of the assigned uncertainty budgets ($\Gamma_k^{DA}, \Gamma_k^{SR,\uparrow}, \Gamma_k^{SR,\downarrow}$). These budgets are defined over the 96 quarter-hourly intervals of the daily horizon and constrain the number of time periods in which the uncertain parameter is allowed to deviate to the level associated with a specific bound k. Crucially, to ensure logical consistency, the summation of budgets across all bounds for a given parameter is limited to 96. This constraint enforces mutual exclusivity, ensuring that any specific time period can be assigned to at most one deviation level. This flexibility allows the operator to shape a less conservative uncertainty distribution—for example, by assigning larger budgets to frequent, minor deviations and restricting extreme deviations to a few rare instances. The uncertainty in DAM electricity prices is characterized by asymmetric intervals, expressed as $\lambda_t^{DA} \in \left[\tilde{\lambda}_t^{DA} - \check{\lambda}_{k,t}^{DA}, \tilde{\lambda}_t^{DA} + \hat{\lambda}_{k,t}^{DA}\right]$, where the magnitudes of positive and negative deviations, $\hat{\lambda}_{k,t}^{DA}$ and $\check{\lambda}_{k,t}^{DA}$, are generally distinct. Within these bounds, the determination of the worst-case price is contingent on the RVPP's net position in the market: a negative deviation constitutes the worst-case scenario when the portfolio is selling energy, whereas a positive deviation represents the worst case during energy purchase intervals. Conversely, for secondary reserve prices, only negative deviations are relevant to the robust analysis, as formulated by the intervals $\left(\lambda_t^{SR,\uparrow} \in \left[\bar{\lambda}_t^{SR,\uparrow} - \check{\lambda}_{k,t}^{SR,\uparrow}, \bar{\lambda}_t^{SR,\uparrow}\right] \text{ and } \lambda_t^{SR,\downarrow} \in \left[\bar{\lambda}_t^{SR,\downarrow} - \check{\lambda}_{k,t}^{SR,\downarrow}, \bar{\lambda}_t^{SR,\downarrow}\right]\right)$. By focusing on these adverse deviations only, the model ensures that the optimization problem accurately reflects the worst-case conditions defined by the chosen uncertainty budgets, ignoring favorable deviations that would increase the RVPP's profit. This modeling choice is consistent with RO theory, in which the inner problem identifies the realization that has the most adverse impact on the objective function or feasibility [42]. The proposed formulation does not discard the favorable side of uncertainty when defining the reference case: for uncertain parameters with a one-sided adverse effect, the favorable bound is used as the reference value and the robust model protects against deviations toward the adverse side. Thus, lower available ND-RES generation, higher demand consumption, lower SRM prices, and the adverse DAM price direction depending on whether the RVPP is selling or buying energy are the critical deviations that determine the robust bidding decision. Favorable deviations are therefore not selected in the inner worst-case problem; explicitly including them in the robust counterpart would not change the robust solution but would increase the size of the formulation.

$$
\begin{aligned}
&\max_{\Xi^F} \left\{ \sum_{t\in\mathcal{T}} \left[\tilde{\lambda}_t^{DA} p_t^{DA} \Delta t + \bar{\lambda}_t^{SR,\uparrow} r_t^{SR,\uparrow} + \bar{\lambda}_t^{SR,\downarrow} r_t^{SR,\downarrow} \right] \right. \\
&- \sum_{t\in\mathcal{T}} \sum_{r\in\mathcal{R}} C_r p_{r,t} \Delta t - \sum_{t\in\mathcal{T}} \sum_{s\in\mathcal{S}} C_s p_{s,t} \Delta t - \sum_{t\in\mathcal{T}} \sum_{c\in\mathcal{C}} C_c p_{c,t} \Delta t \\
&- \max_{\left\{\mathcal{T}_k^{DA}, \mathcal{T}_k^{SR,\uparrow}, \mathcal{T}_k^{SR,\downarrow}\right\}} \left\{ \sum_{t\in\mathcal{T}_k^{DA}} \sum_{k\in\mathcal{K}} \check{\lambda}_{k,t}^{DA} y_{k,t}^{DA} + \sum_{t\in\mathcal{T}_k^{SR,\uparrow}} \sum_{k\in\mathcal{K}} \check{\lambda}_{k,t}^{SR,\uparrow} r_t^{SR,\uparrow} \right. \\
&\left. \left. + \sum_{t\in\mathcal{T}_k^{SR,\downarrow}} \sum_{k\in\mathcal{K}} \check{\lambda}_{k,t}^{SR,\downarrow} r_t^{SR,\downarrow} \right\} \right\}
\end{aligned}
\tag{8}
$$

The constraints governing the proposed bi-level MBRO framework are detailed in (9). Constraint (9a) addresses the asymmetric characteristics of DAM price uncertainty through the positive auxiliary variable $y_{k,t}^{DA}$. By distinguishing between positive ($\hat{\lambda}_{k,t}^{DA}$) and negative ($\check{\lambda}_{k,t}^{DA}$) price deviations, this variable effectively models the worst-case price realization contingent on the direction of the RVPP's energy trade in each period [32]. The uncertainty associated with ND-RES generation and demand consumption is managed by Eqs. (9b) and (9c), respectively. These constraints incorporate specific uncertainty bounds to account for scenarios that worsen the objective function: ND-RES production is modeled with a focus on potential negative deviations $\left(P_{r,t} \in [\bar{P}_{r,t} - \check{P}_{r,k,t}, \bar{P}_{r,t}]\right)$, whereas demand is modeled to account for potential positive deviations $\left(P_{d,t} \in [\underline{P}_{d,t}, \underline{P}_{d,t} + \hat{P}_{d,k,t}]\right)$. The worst-case realizations for these parameters are determined by inner-level maximization problems performed over the sets $\mathcal{T}_{r,k}$ and $\mathcal{T}_{d,k}$, whose cardinalities, as discussed earlier, are equal to the uncertainty budgets $\Gamma_{r,k}$ and $\Gamma_{d,k}$ for each bound k. Consequently, constraints (9b) and (9c) apply the respective deviations (i.e., to reduce $\check{P}_{r,k,t'}$ and/or to increase $\hat{P}_{d,k,t'}$) to the forecast reference only if the index t' matches the current period t and simultaneously belongs to the selected worst-case set (i.e., $t' = t$ and $t' \in \mathcal{T}_{r,k}$ or $t' \in \mathcal{T}_{d,k}$). Finally, all deterministic constraints from Section 3.1 that remain unchanged under uncertainty are integrated in (9d).

$$
-\frac{\check{\lambda}_{k,t}^{DA}}{\hat{\lambda}_{k,t}^{DA}} y_{k,t}^{DA} \le p_t^{DA} \Delta t \le y_{k,t}^{DA} \; ; \qquad \forall k,t \in \mathcal{K},\mathcal{T} \tag{9a}
$$

$$
p_{r,t} + r_{r,t}^{\uparrow} \le \bar{P}_{r,t} - \max_{\{\mathcal{T}_{r,k}\}} \left\{ \sum_{t'\in\mathcal{T}_{r,k}, t'=t} \sum_{k\in\mathcal{K}} \check{P}_{r,k,t'} \right\} ; \qquad \forall r,t \in \mathcal{R},\mathcal{T} \tag{9b}
$$

$$
p_{d,t} - r_{d,t}^{\uparrow} \ge \underline{P}_{d,t} + \max_{\{\mathcal{T}_{d,k}\}} \left\{ \sum_{t'\in\mathcal{T}_{d,k}, t'=t} \sum_{k\in\mathcal{K}} \hat{P}_{d,k,t'} \right\} ; \qquad \forall d,t \in \mathcal{D},\mathcal{T} \tag{9c}
$$

$$
(2), (3), (4b), (5b)–(5c), (6), (7) \; ; \tag{9d}
$$

3.2.2. Inner problems reformulation

The maximization term in the third line of the objective function (8) (the protection function) conceptually identifies the worst-case scenario via time sets $\mathcal{T}_k^{DA}, \mathcal{T}_k^{SR,\uparrow}, \mathcal{T}_k^{SR,\downarrow}$; however, since these sets are not predetermined, their selection logic must be recast as an equivalent linear optimization problem to facilitate the derivation of the final robust formulation [38]. Specifically, set membership is represented through positive auxiliary variables in the linear problem, whose optimal values yield the same worst-case choice as the original set-based definition by limiting their allowable deviations across time periods and within each bound. To achieve this, by treating the optimal values of the upper-level variables ($y_{k,t}^{DA^*}$, $r_t^{SR,\uparrow^*}$, $r_t^{SR,\downarrow^*}$) as fixed parameters in the lower-level problem and applying Proposition 1 (see Appendix A), the protection function in (8) is transformed into the linear problem (10). In this formulation, constraints (10b)–(10d) restrict the summation of each of the positive auxiliary variables $z_{k,t}^{DA}$, $z_{k,t}^{SR,\uparrow}$, and $z_{k,t}^{SR,\downarrow}$ over all time periods for each uncertainty bound k to the corresponding uncertainty budgets Γ_k^{DA}, $\Gamma_k^{SR,\uparrow}$, and $\Gamma_k^{SR,\downarrow}$, respectively. Simultaneously, constraints (10e)–(10g) ensure that the summation of these auxiliary variables across all bounds for any given time period does not exceed 1. This linear structure mathematically replicates the mutual exclusivity of the worst-case sets, ensuring that the optimal value of (10a) matches the protection function in (8). The dual variables associated with each constraint are defined alongside these equations and are subsequently utilized in Section 3.2.3 to derive the final MILP formulation.

$$
\begin{aligned}
\max \Bigg\{ &\sum_{t\in\mathcal{T}} \sum_{k\in\mathcal{K}} \check{\lambda}_{k,t}^{DA} y_{k,t}^{DA^*} z_{k,t}^{DA} + \sum_{t\in\mathcal{T}} \sum_{k\in\mathcal{K}} \check{\lambda}_{k,t}^{SR,\uparrow} r_t^{SR,\uparrow^*} z_{k,t}^{SR,\uparrow} \\
&+ \sum_{t\in\mathcal{T}} \sum_{k\in\mathcal{K}} \check{\lambda}_t^{SR,\downarrow} r_t^{SR,\downarrow^*} z_{k,t}^{SR,\downarrow} \Bigg\}
\end{aligned}
\tag{10a}
$$

st.

$$\sum_{t\in\mathcal{T}} z^{DA}_{k,t} \le \Gamma^{DA}_{k} \;:\; \phi^{DA}_{k} \;; \qquad \forall k\in\mathcal{K} \qquad (10b)$$

$$\sum_{t\in\mathcal{T}} z^{SR,\uparrow}_{k,t} \le \Gamma^{SR,\uparrow}_{k} \;:\; \phi^{SR,\uparrow}_{k} \;; \qquad \forall k\in\mathcal{K} \qquad (10c)$$

$$\sum_{t\in\mathcal{T}} z^{SR,\downarrow}_{k,t} \le \Gamma^{SR,\downarrow}_{k} \;:\; \phi^{SR,\downarrow}_{k} \;; \qquad \forall k\in\mathcal{K} \qquad (10d)$$

$$0 \le \sum_{k\in\mathcal{K}} z^{DA}_{k,t} \le 1 \;:\; \zeta^{DA}_{t} \;; \qquad \forall t\in\mathcal{T} \qquad (10e)$$

$$0 \le \sum_{k\in\mathcal{K}} z^{SR,\uparrow}_{k,t} \le 1 \;:\; \zeta^{SR,\uparrow}_{t} \;; \qquad \forall t\in\mathcal{T} \qquad (10f)$$

$$0 \le \sum_{k\in\mathcal{K}} z^{SR,\downarrow}_{k,t} \le 1 \;:\; \zeta^{SR,\downarrow}_{t} \;; \qquad \forall t\in\mathcal{T} \qquad (10g)$$

The protection function describing the uncertainty of ND-RES electrical production in constraint (9b) (the maximization term on the right-hand side) is recast as the linear formulation (11) by applying Proposition 2 (see Appendix A). To achieve the same worst-case selection logic as in (9b), the optimization problem (11) is defined individually for each time period t and ND-RES unit r [32]. The objective function (11a) maximizes the production deviation for the current period $t' = t$. Constraint (11b) ensures that the sum of the auxiliary variable $z_{r,k,(t'=t)}$ for the current period and the aggregate optimal values of variables from other protection functions ($z^{*}_{r,k,t'}$ where $t' \neq t$) remains within the limit $\Gamma_{r,k}$. Note that the variables $z^{*}_{r,k,t'}$ correspond to other protection functions (where $t' \neq t$) and are therefore treated as parameters in this constraint. Furthermore, the summation of the auxiliary variable $z_{r,k,(t'=t)}$ across all uncertainty bounds is limited to 1 by constraint (11c). The equivalent linear formulation for the demand uncertainty protection function in constraint (9c) follows an identical derivation and is omitted here for brevity.

$$\max \sum_{k\in\mathcal{K}} \check{P}_{r,k,(t'=t)}\, z_{r,k,(t'=t)} \;; \qquad \forall r,t\in\mathcal{R},\mathcal{T} \qquad (11a)$$

st.

$$z_{r,k,(t'=t)} + \sum_{t'\neq t} z^{*}_{r,k,t'} \le \Gamma_{r,k} \;:\; \phi_{r,k} \;; \qquad \forall k\in\mathcal{K} \qquad (11b)$$

$$0 \le \sum_{k\in\mathcal{K}} z_{r,k,(t'=t)} \le 1 \;:\; \zeta_{r,t} \;; \qquad (11c)$$

3.2.3. MILP formulation

By leveraging strong duality theory [43], the inner linear maximization problems defined in (10) and (11) (as well as the analogous formulation for demand uncertainty) are replaced by their respective dual problems. Substituting the dual forms directly into the objective function (8) and constraints (9b) and (9c) yields the final single-level MILP formulation presented in (12). In this formulation, the objective function (12a) retains the deterministic profit terms in its first two lines, while the third line explicitly penalizes the objective function for the worst-case revenue losses arising from DAM and SRM price uncertainties. The dual expression in the third line of (12a) is the single-level equivalent of the worst-case protection functions in (8). Accordingly, this term has the same economic interpretation as the robust cost defined in Section 3.2.1. Constraint (12c) replicates the asymmetric price logic from (9a), and constraints (12d)–(12f) enforce the dual restrictions corresponding to the price uncertainty problem defined in (10).

The worst-case limits for ND-RES production are governed by constraints (12g)–(12k). Specifically, constraint (12g) defines the robust production upper bound. To model the discrete logical condition where the remaining budget term ($\Gamma_{r,k} - \sum_{t'\neq t} z^{*}_{r,k,t'}$) only corresponds to 0 or 1, the binary variable $\chi_{r,k,t}$ is introduced. Consequently, the positive auxiliary variable $y_{r,k,t}$ is established in (12g) and bounded via constraint (12h) using the Big-M method [43], thus linearizing the dual term $\sum_{k\in\mathcal{K}} \chi_{r,k,t}\phi_{r,k} + \zeta_{r,t}$. To ensure logical consistency, constraint (12i) enforces mutual exclusivity, ensuring only one uncertainty bound is active per time period, while constraint (12j) ensures the total number of active worst-case periods for each bound k matches the assigned uncertainty budget. Constraint (12k) represents the standard dual constraints derived from the ND-RES protection function (11). Similarly, constraints (12l)–(12p) manage demand uncertainty. These follow the same structural logic as the ND-RES constraints, with the primary distinction being the direction of the worst-case deviation. The domains of all positive auxiliary variables are defined in (12q)–(12r), and the remaining deterministic constraints are consolidated in (12s). Critically, this refined MILP framework allows for the flexible management of multiple uncertainty sources and enables the selection of distinct conservatism levels across different bounds via the uncertainty budgets.

$$\max_{\Xi^{F},\Xi^{S}} \Bigg\{ \sum_{t\in\mathcal{T}} \left[\bar{\lambda}^{DA}_{t} p^{DA}_{t} \Delta t + \bar{\lambda}^{SR,\uparrow}_{t} r^{SR,\uparrow}_{t} + \bar{\lambda}^{SR,\downarrow}_{t} r^{SR,\downarrow}_{t} \right] \qquad (12a)$$

$$- \sum_{t\in\mathcal{T}}\sum_{r\in\mathcal{R}} C_{r} p_{r,t}\Delta t - \sum_{t\in\mathcal{T}}\sum_{s\in\mathcal{S}} C_{s} p_{s,t}\Delta t - \sum_{t\in\mathcal{T}}\sum_{c\in\mathcal{C}} C_{c} p_{c,t}\Delta t$$

$$- \sum_{k\in\mathcal{K}} \left[\Gamma^{DA}_{k}\phi^{DA}_{k} + \Gamma^{SR,\uparrow}_{k}\phi^{SR,\uparrow}_{k} + \Gamma^{SR,\downarrow}_{k}\phi^{SR,\downarrow}_{k} \right] - \sum_{t\in\mathcal{T}} \left[\zeta^{DA}_{t} + \zeta^{SR,\uparrow}_{t} + \zeta^{SR,\downarrow}_{t} \right] \Bigg\} \qquad (12b)$$

st.

$$-\frac{\check{\lambda}^{DA}_{k,t}}{\hat{\lambda}^{DA}_{k,t}} y^{DA}_{k,t} \le {p_{t}}^{DA}\Delta t \le y^{DA}_{k,t} \;; \qquad \forall k,t\in\mathcal{K},\mathcal{T} \qquad (12c)$$

$$\phi^{DA}_{k} + \zeta^{DA}_{t} \ge \check{\lambda}^{DA}_{k,t} y^{DA}_{k,t} \;; \qquad \forall k,t\in\mathcal{K},\mathcal{T} \qquad (12d)$$

$$\phi^{SR,\uparrow}_{k} + \zeta^{SR,\uparrow}_{t} \ge \check{\lambda}^{SR,\uparrow}_{k,t} r^{SR,\uparrow}_{t} \;; \qquad \forall k,t\in\mathcal{K},\mathcal{T} \qquad (12e)$$

$$\phi^{SR,\downarrow}_{k} + \zeta^{SR,\downarrow}_{t} \ge \check{\lambda}^{SR,\downarrow}_{k,t} r^{SR,\downarrow}_{t} \;; \qquad \forall k,t\in\mathcal{K},\mathcal{T} \qquad (12f)$$

$$p_{r,t} + r^{\uparrow}_{r,t} \le \bar{P}_{r,t} - \sum_{k\in\mathcal{K}} \chi_{r,k,t}\,\phi_{r,k} - \zeta_{r,t} = \bar{P}_{r,t} - \sum_{k\in\mathcal{K}} y_{r,k,t} \;; \qquad \forall r,t\in\mathcal{R},\mathcal{T} \qquad (12g)$$

$$\phi_{r,k} + \zeta_{r,t} - M(1-\chi_{r,k,t}) \le y_{r,k,t} \le M\chi_{r,k,t} \;; \qquad \forall r,k,t\in\mathcal{R},\mathcal{K},\mathcal{T} \qquad (12h)$$

$$\sum_{k\in\mathcal{K}} \chi_{r,k,t} \le 1 \;; \qquad \forall r,t\in\mathcal{R},\mathcal{T} \qquad (12i)$$

$$\sum_{t\in\mathcal{T}} \chi_{r,k,t} = \Gamma_{r,k} \;; \qquad \forall r,k\in\mathcal{R},\mathcal{K} \qquad (12j)$$

$$\phi_{r,k} + \zeta_{r,t} \ge \check{P}_{r,k,t} \;; \qquad \forall r,k,t\in\mathcal{R},\mathcal{K},\mathcal{T} \qquad (12k)$$

$$p_{d,t} - r^{\uparrow}_{d,t} \ge \underline{P}_{d,t} + \sum_{k\in\mathcal{K}} \chi_{d,k,t}\,\phi_{d,k} + \zeta_{d,t} = \underline{P}_{d,t} + \sum_{k\in\mathcal{K}} y_{d,k,t} \;; \qquad \forall d,k,t\in\mathcal{D},\mathcal{K},\mathcal{T} \qquad (12l)$$

$$\phi_{d,k} + \zeta_{d,t} - M(1-\chi_{d,k,t}) \le y_{d,k,t} \le M\chi_{d,k,t} \;; \forall d,k,t\in\mathcal{D},\mathcal{K},\mathcal{T} \qquad (12m)$$

$$\sum_{k\in\mathcal{K}} \chi_{d,k,t} \le 1 \;; \qquad \forall d,t\in\mathcal{D},\mathcal{T} \qquad (12n)$$

$$\sum_{t\in\mathcal{T}} \chi_{d,k,t} = \Gamma_{d,k} \;; \qquad \forall d,k\in\mathcal{D},\mathcal{K} \qquad (12o)$$

$$\phi_{d,k} + \zeta_{d,t} \ge \hat{P}_{d,k,t} \;; \qquad \forall d,k,t\in\mathcal{D},\mathcal{K},\mathcal{T} \qquad (12p)$$

$$\phi^{DA}_{k}, \phi^{SR,\uparrow}_{k}, \phi^{SR,\downarrow}_{k}, \zeta^{DA}_{t}, \zeta^{SR,\uparrow}_{t}, \zeta^{SR,\downarrow}_{t}, y^{DA}_{k,t} \ge 0 \;; \qquad \forall k,t\in\mathcal{K},\mathcal{T} \qquad (12q)$$

$$\phi_{r,k}, \phi_{d,k}, \zeta_{r,t}, \zeta_{d,t}, y_{r,k,t}, y_{d,k,t} \ge 0 \;; \qquad \forall r,d,k,t\in\mathcal{R},\mathcal{D},\mathcal{K},\mathcal{T} \qquad (12r)$$

(2), (3), (4b), (5b)–(5c), (6), (7) ; (12s)

Fig. 2 summarizes the overall workflow of the approach presented in this section: it outlines the deterministic RVPP formulation and the main steps leading to the MBRO model and its final single-level MILP. The figure also highlights the key characteristics enabled by the MBRO approach. The advantages of this proposed MBRO approach—specifically

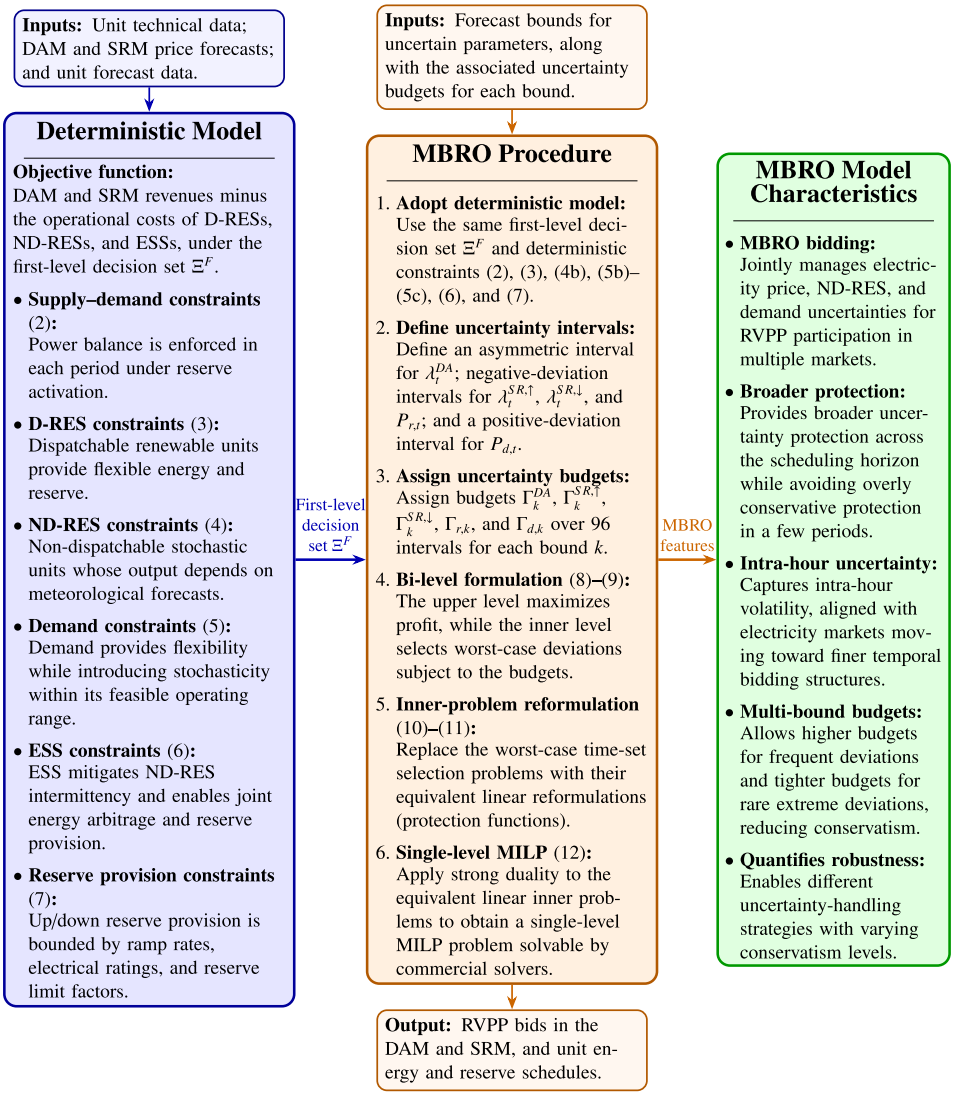


Fig. 2. Procedure for developing the proposed MBRO framework and its key characteristics.

its ability to yield less conservative and more realistic solutions compared to classical robust optimization—are rigorously validated through the case studies presented in Section 4.

4. Case studies

This section presents and discusses simulation results obtained with the proposed MBRO framework, with the aim of assessing how multiple sources of uncertainty affect the performance of an RVPP participating in the DAM and SRM. All experiments were executed on a Dell XPS laptop (Intel i7-1165G7, 2.8 GHz, 16 GB RAM) using CPLEX within GAMS 39.1.1.

4.1. System description and model parametrization

To account for the heterogeneity of the assets that may comprise an RVPP, and without loss of generality, the case study considers an RVPP located in Spain composed of a hydro plant, a wind farm, a solar PV plant, a Li-ion ESS, and a demand unit. The considered portfolio is a representative test RVPP rather than one specific operating plant. The rated capacities are selected to provide a balanced aggregation of different resource types for comparing the proposed and benchmark uncertainty-handling models. In particular, the same rated value of 50 MW is assigned to the solar PV plant, wind farm, and flexible demand so that the comparison is not dominated by one specific asset type. The technology-specific behavior is captured through the corresponding generation/consumption profiles, operational limits, and uncertainty bounds. Forecast data for the uncertain inputs, namely wind and solar PV generation, demand consumption, DAM electricity prices, and up/down SRM prices, are derived from Spanish historical records reported by [44]. The numerical analysis considers two representative periods, November 2025 and spring 2026, to assess whether the qualitative findings of the proposed MBRO approach remain consistent under different seasonal conditions, particularly with respect to renewable-generation patterns, demand levels, and market-price behavior. Although the analysis focuses on two representative periods, the proposed framework is not tied to these specific windows and can be readily applied to longer datasets as additional quarter-hourly market data become available for Spain. The corresponding uncertainty bounds are illustrated in Fig. 3. For each uncertain parameter, three bounds ($k = 1, 2, 3$) are defined: $k = 1$ represents the most likely deviation range around the forecast, while $k = 2$ and $k = 3$ capture progressively less likely (more extreme) deviations, depicted with lighter shading. The uncertainty bounds and their associated budgets are specified using complementary criteria. The uncertainty bounds are calibrated from

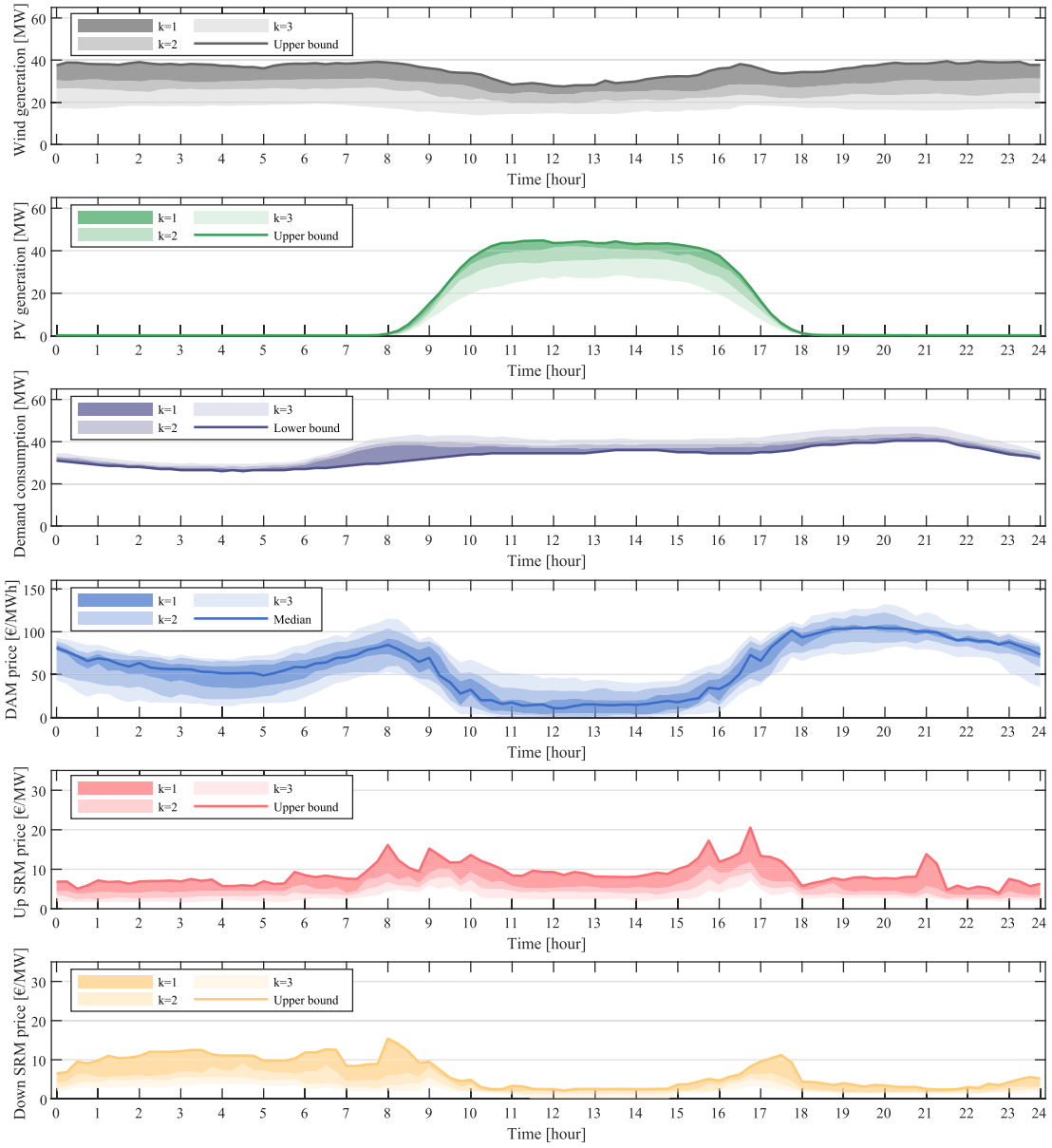


Fig. 3. Uncertainty bounds in multi-bound for different uncertainty-handling strategies.

historical forecast-error distributions, whereas the budgets are operator-defined robustness settings used to represent different risk preferences. The detailed calibration of the uncertainty bounds and the selection of the corresponding budgets are explained in Section 4.2.

The technical characteristics of the RVPP assets are summarized in Table 2 and are taken from [31,32]. Table 3 reports the uncertainty budgets associated with the bounds in Fig. 3 for: (i) the proposed MBRO model with a 15-minute bidding resolution, (ii) a classic RO model with 15-minute resolution, and (iii) an RO model with hourly resolution. For each uncertainty-handling strategy, the budget settings reported in Table 3 are applied uniformly across all uncertain parameters within each corresponding robust framework. In the MBRO formulation, the sum of the budgets over all bounds ($k = 1, 2, 3$) is constrained to lie within 0 to 96. In the RO model with 15-minute resolution, the budget varies from 0 to 96, where larger values represent more conservative operation by allowing more periods to reach their worst-case realizations. In the hourly RO model, the corresponding budget ranges from 0 to 24, spanning the deterministic case (0) to the most conservative case (24), in which all hours may simultaneously attain worst-case values.

To further compare the proposed MBRO framework with another robustness-based uncertainty-handling method, a data-driven Wasserstein-DRO benchmark based on the general framework in [45] is also implemented. In this model, the DAM energy bid, the upward and downward SRM reserve bids, and the unit-level scheduling decisions are treated as here-and-now decisions that are common to all scenarios. The empirical distribution is constructed from 92 complete historical daily trajectories, each comprising 96 consecutive 15-minute periods, with equal probability assigned to all trajectories. For each trajectory, the DAM price, upward and downward SRM prices, wind and solar PV generation, and demand are retained jointly using their original historical timestamps. Consequently, the temporal dependence within each day and the observed cross-variable dependence among the uncertain quantities are preserved. The realized market prices determine the scenario market revenue, while deviations in renewable generation and demand

Table 2
RVPP units data.

Parameter	Solar PV	Wind farm	Hydro	ESS	Demand
$\bar{P}_u/\underline{P}_u$ [MW]	50/0	50/0	50/10	–	50/0
$R_u^{\uparrow}/R_u^{\downarrow}$ [MW/min]	20/25	15/20	10/10	10/10	3/3
$\beta_u^{\uparrow}/\beta_u^{\downarrow}$ [%]	5	5	50	100	0
$\bar{E}_u/\underline{E}_u$ [MWh]	–	–	480/-	30/3	-/750
$\bar{P}_s^{+}/\bar{P}_s^{-}$ [MW]	–	–	–	10/10	–
η_s^{+}/η_s^{-} [%]	–	–	–	95/95	–
C_u [€/MWh]	10	15	12.5	30	–

Table 3
Uncertainty budgets for the RVPP operator's strategies in different robust frameworks.

	MBRO			RO 15-min	RO hourly
Strategy	k = 1	k = 2	k = 3		
Optimistic	16	4	2	16	4
Balanced	32	8	4	32	8
Pessimistic	48	12	6	48	12

determine the corresponding imbalance settlement. The objective maximizes the scenario-weighted net market revenue, including imbalance settlement, minus the operating cost and the Wasserstein penalty associated with the three market-specific radii. The complete mathematical formulation is provided in Appendix B.

The Wasserstein radii and the shortage-penalty multiplier are tuned separately because they affect different terms of the benchmark objective. Using the 92-day calibration dataset, the historical relationship between the DAM and upward imbalance prices is examined to establish an economically plausible range for the shortage-penalty multiplier ρ^{-}. Three values spanning this range are assigned to the optimistic, balanced, and pessimistic strategies to represent increasing aversion to energy shortages, while $\rho^{+} = 0$ for all strategies. The market-specific radii ϵ^{DA}, $\epsilon^{SR,\uparrow}$, and $\epsilon^{SR,\downarrow}$ are tuned jointly through a sensitivity analysis using the same calibration dataset. For each candidate triplet, the resulting Wasserstein cost and energy and reserve bidding levels are examined. Representative triplets that provide the intended monotonic ordering of conservatism are selected for the optimistic, balanced, and pessimistic strategies, respectively. Separate radii are used to control the ambiguity associated with the DAM, upward-SRM, and downward-SRM price distributions independently. The selected values, reported in Table 4, define three differentiated levels of conservatism rather than unique statistical estimates.

This section further examines the computational performance of the proposed model using an enlarged RVPP consisting of 23 units. The enlarged portfolio includes two hydro plants, six wind farms, six solar PV plants, three Li-ion ESSs, and six demand units. The corresponding input data are obtained by applying specific adjustments to the unit data of the *original* RVPP described previously.

Table 4
Main parameters of the Wasserstein-DRO benchmark under different uncertainty-handling strategies.

Strategy	N_s [–]	ϵ^{DA} [€/MWh]	$\epsilon^{SR,\uparrow}$ [€/MW]	$\epsilon^{SR,\downarrow}$ [€/MW]	ρ^{-} [pu]
Optimistic	92	2.0	1.5	0.2	2.0
Balanced	92	6.0	2.5	0.4	3.0
Pessimistic	92	8.0	3.5	0.6	4.0

N_s is the number of DRO scenarios. Parameters ϵ^{DA}, $\epsilon^{SR,\uparrow}$, and $\epsilon^{SR,\downarrow}$ denote the Wasserstein radii associated with day-ahead energy, upward reserve, and downward reserve prices, respectively. Parameter ρ^{-} is the shortage-penalty multiplier applied to the day-ahead market price for energy shortage, while the surplus-energy multiplier ρ^{+} is fixed at zero.

Based on the above budgets and benchmark settings, four strategies are considered for the RVPP operator: a deterministic strategy and three uncertainty-handling strategies, namely optimistic, balanced, and pessimistic. The following case studies are used to quantify the impact of the proposed MBRO approach, benchmark it against alternative robust frameworks, examine the effect of market time resolution, and assess the practical performance of the obtained bidding decisions:

- **Case 1:** Evaluate the optimal operation of the RVPP units under the proposed MBRO model for the deterministic, optimistic, balanced, and pessimistic strategies.
- **Case 2:** Compare RVPP trading outcomes in the DAM and SRM using the classic single-bound RO model under hourly and 15-minute market resolutions across the different bidding strategies considered.
- **Case 3:** Compare the classic single-bound RO, proposed MBRO, and Wasserstein-DRO approaches in terms of economic results, traded energy, traded reserve, and uncertainty-handling behavior. This case also includes the additional computational-performance assessment of the proposed model for both the original 5-unit RVPP and the enlarged 23-unit RVPP.
- **Case 4:** Perform a sensitivity analysis on the uncertainty budgets of the proposed MBRO framework. Four subcases are considered to separately examine the impact of the inner, intermediate, and outer uncertainty bounds, as well as the combined effect of increasing all uncertainty budgets.
- **Case 5:** Conduct an out-of-sample assessment of the bidding decisions obtained from the classic single-bound RO, proposed MBRO, and Wasserstein-DRO approaches. This case evaluates the realized profit and imbalance cost under held-out historical realizations, thereby assessing the implementability of the obtained schedules.

4.2. Calibration of uncertainty bounds and selection of budgets

To make the construction of the MBRO uncertainty bounds reproducible, a percentile-based calibration procedure is adopted. For each uncertain parameter and each 15-minute period, historical observations from the corresponding seasonal dataset are collected. The nested bounds are then obtained from empirical percentiles of these observations. For the DAM price, the median value is used as the reference value, and the lower/upper percentile pairs 25%/75%, 10%/90%, and 2%/98% are used to define the three bounds $k = 1$, $k = 2$, and $k = 3$, respectively. This percentile selection creates a decreasing-frequency structure, where the inner bound represents frequent moderate deviations and the outer bound represents rare extreme deviations. For ND-RES generation and upward/downward SRM prices, the upper percentile is used as the deterministic reference value, and lower percentiles are used to define adverse downward deviations. For demand, the lower reference value is used, and upward deviations are constructed from higher percentiles. Fig. 4 illustrates the uncertainty-bound calibration procedure for the DAM price; the same calibration logic is applied to the other uncertain parameters.

The uncertainty budgets are selected separately from the percentile-calibrated uncertainty bounds and determine how many 15-minute periods may experience the adverse deviation level associated with each bound. Historical information on the expected frequency and severity of deviations can inform their selection, but the budgets are not obtained by directly matching the number of protected periods to historical exceedance counts. In the proposed multi-bound structure, a larger budget can be assigned to the inner bound to provide broader protection against moderate deviations across the scheduling horizon, whereas smaller budgets are assigned to the intermediate and outer bounds to limit the number of periods exposed to increasingly severe deviations. Accordingly, the budgets are selected such that $\Gamma_{k=1} \geq \Gamma_{k=2} \geq \Gamma_{k=3}$. In addition, larger budgets are assigned to the more conservative uncertainty-handling strategies. The representative values reported

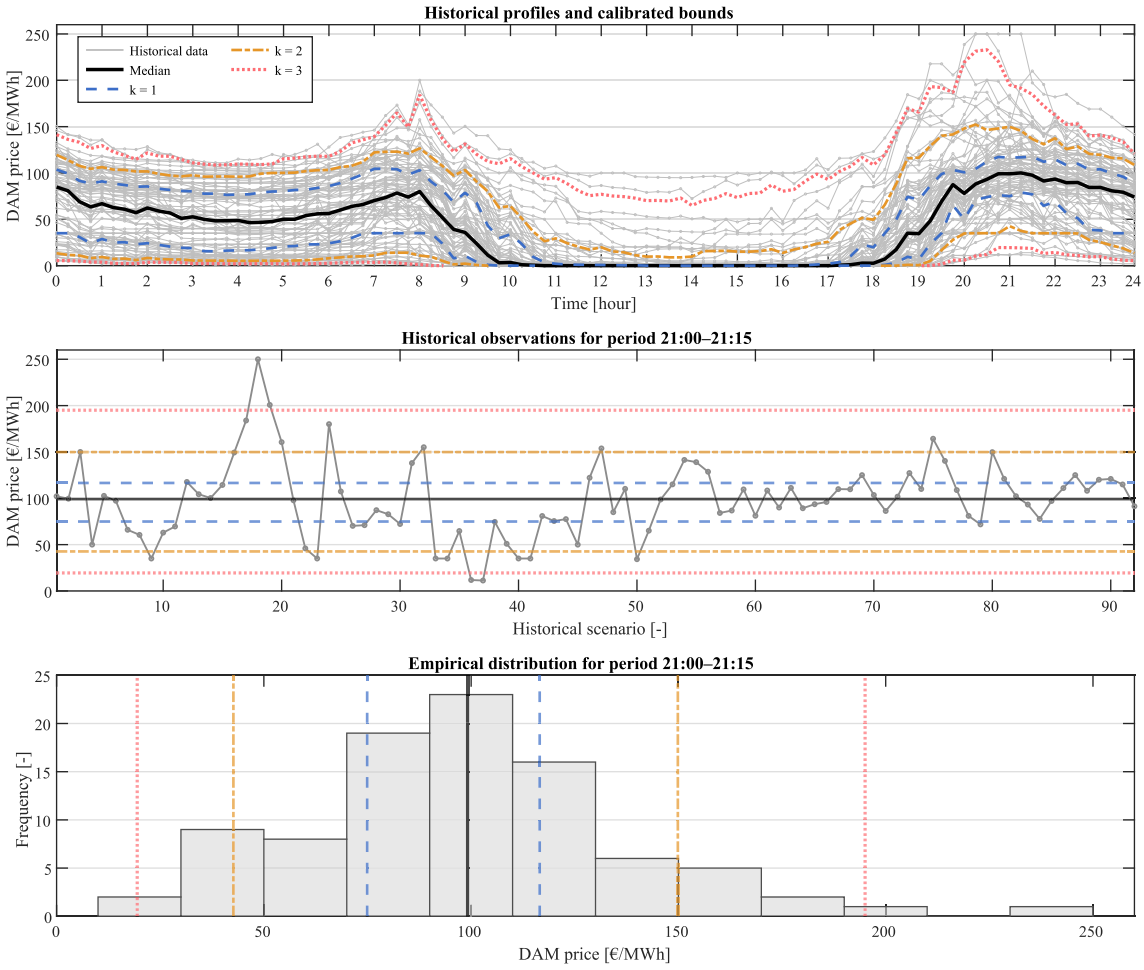


Fig. 4. Calibration of the multi-bound uncertainty set for the DAM price using spring-season data.

in Table 3 therefore define optimistic, balanced, and pessimistic levels of conservatism. Since the appropriate budget allocation depends on the desired balance between robustness and economic performance, alternative allocations are evaluated through the sensitivity analysis in Section 4.6. The results show that increasing the outer-bound budget has a stronger effect on profit and traded energy than increasing the inner-bound budget, supporting the use of broader protection against moderate deviations and more limited protection against the most severe deviations.

4.3. Case 1

Fig. 5 shows the energy schedules of the different RVPP units under a 15-minute market resolution for the different bidding strategies considered. In the deterministic strategy, the forecast values are treated as exact and uncertainties are neglected in the optimization problem, yielding the optimal unit dispatch under perfect-forecast assumptions. Wind and solar PV supply energy in the DAM according to their availability. In addition, the dispatchable hydro unit mainly generates during periods with high DAM prices, i.e., around 00:00–01:30, 06:45–08:45, and 16:45–24:00 (see the electricity price in Fig. 3). The ESS charges mainly between 11:15 and 13:45, when solar PV availability is high, and discharges between 19:00 and 20:30, when DAM prices are higher. Under the optimistic strategy, uncertain parameters are allowed to deviate from their deterministic reference values according to uncertainty budgets defined in Table 3. Consequently, the scheduled energy of the units is affected, with lower wind and solar PV generation and higher demand consumption in the worst case. To compensate for the reduced output of the ND-RES, the hydro plant is scheduled for more periods than in the deterministic strategy. For instance, hydro generation extends over 00:00–01:45, 06:15–09:15, and 17:00–24:00. For the more conservative balanced and pessimistic strategies, the RVPP operator accounts for higher volatility in ND-RES when determining the unit schedules. As expected, the RVPP trades lower energy in the DAM, with greater variability across periods. Moreover, the role of the hydro plant in mitigating ND-RES fluctuations becomes more pronounced, and this dispatchable unit is scheduled more frequently. For example, under the pessimistic strategy, hydro generation is scheduled over 00:00–02:30, 05:30–09:15, and 16:45–24:00. Additionally, under the pessimistic strategy, the ESS schedules charging and discharging over a wider time window than in the deterministic strategy to hedge against uncertainty. For example, the ESS charges during 11:30–14:45 and discharges during 18:45–21:30. Overall, the results in Fig. 5 indicate that the proposed framework effectively captures the impact of uncertainty on RVPP scheduling at a 15-minute market resolution across different uncertainty-handling strategies.

Fig. 6 shows the shares of up and down reserve provided by the RVPP units under a 15-minute market resolution for different bidding strategies. The results indicate that the ESS is one of the main providers of up reserve in the SRM. For instance, under the deterministic strategy, the ESS provides up reserve during several periods around 08:00–10:15, 15:30–17:30, and 21:00–21:15, when the up-SRM price is high (see Fig. 3). A smaller share of up reserve is provided by the wind farm and the solar PV plant, mainly between 10:15 and 15:45. Regarding down reserve in the deterministic strategy, most of the down reserve is supplied

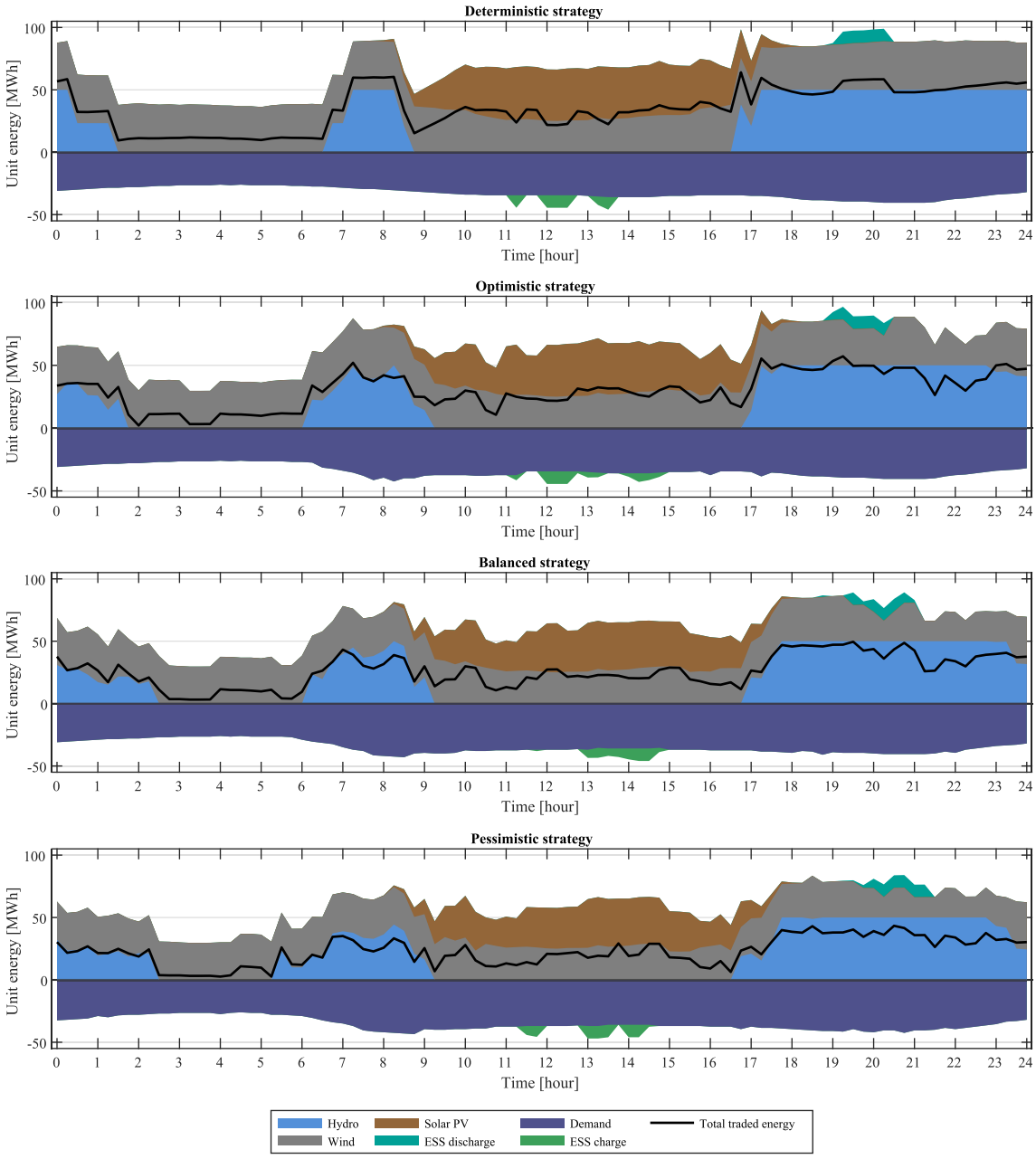


Fig. 5. Case 1 – All RVPP unit energy in multi-bound for different uncertainty-handling strategies.

by the hydro plant during the hours in which it is generating and can therefore curtail its output to provide down reserve. The ESS also provides down reserve in some periods, for example between 02:15 and 06:45. In addition, the wind farm and solar PV contribute a small share of down reserve depending on their availability to reduce production. It is worth noting that providing down reserve is generally easier than providing up reserve; accordingly, the RVPP offers down reserve in almost all scheduling periods. In contrast, up reserve is offered in fewer periods because the RVPP often prefers to allocate its resources to DAM energy trading rather than to up-reserve provision. Moreover, since DAM electricity prices are typically higher than SRM prices, energy trading tends to be a more reliable revenue source for the RVPP. Nevertheless, the RVPP still arbitrages between the two markets to enhance profitability. When adopting the optimistic strategy, and especially the more conservative balanced and pessimistic strategies, the RVPP tends to provide up reserve over a larger number of periods, typically with a lower reserve magnitude per period compared with the deterministic strategy. This behavior can be explained by the fact that, once uncertainty is explicitly considered in the proposed MBRO framework, SRM prices may be adversely affected across many periods. Consequently, the RVPP adopts a more diversified reserve-bidding profile over time, reducing its exposure to price fluctuations in any single period and leading to a more robust and risk-averse strategy for profit maximization.

4.4. Case 2

Fig. 7 compares the RVPP trading outcomes obtained with the *classic* RO model under hourly and 15-minute market resolutions across different uncertainty-handling strategies. Overall, the 15-minute formulation captures intra-hour trading dynamics that are inherently smoothed in the hourly framework, leading to more realistic and granular bidding decisions. Adopting alternative uncertainty-handling strategies can even

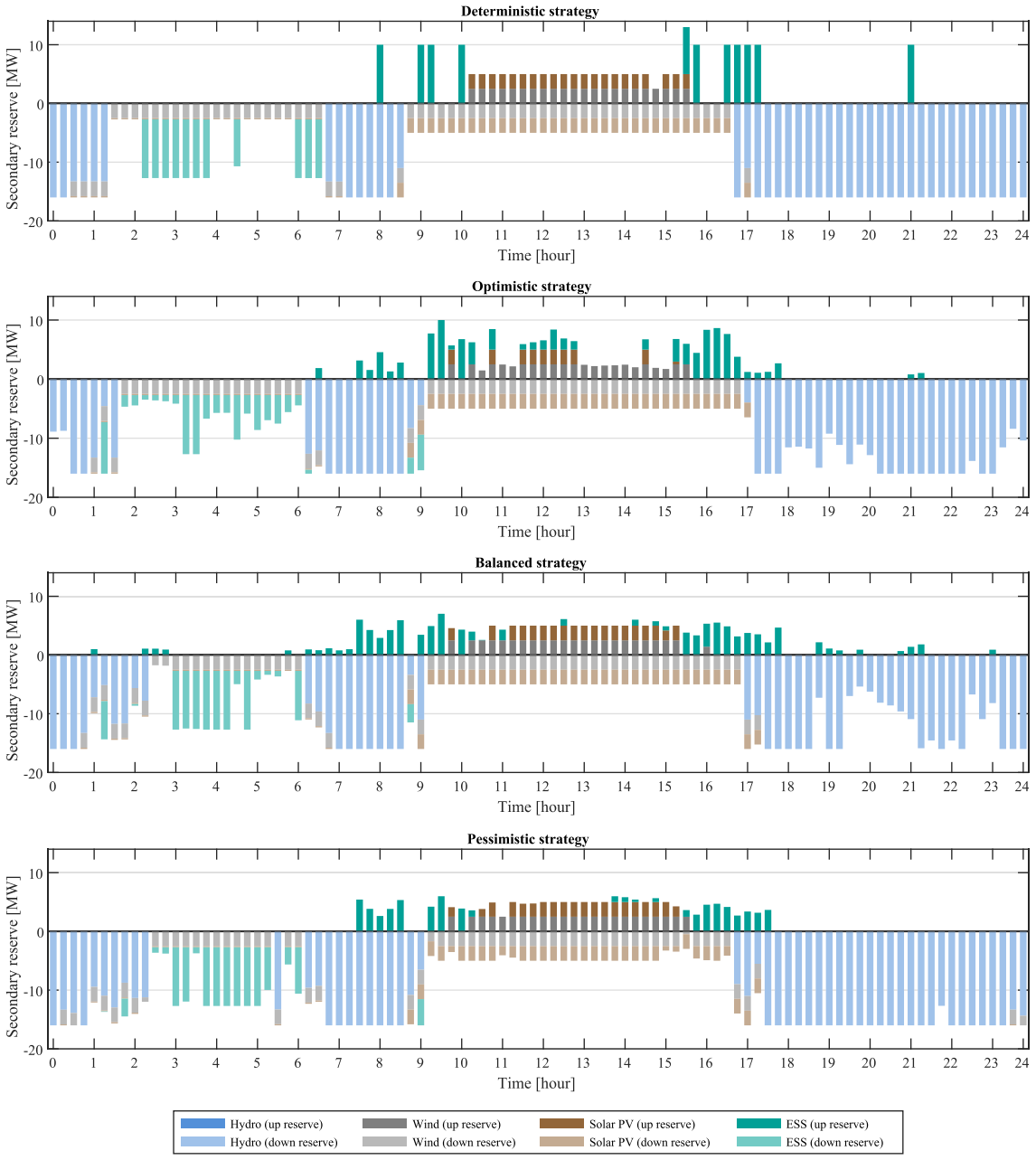


Fig. 6. Case 1 – All RVPP unit reserves in multi-bound for different uncertainty-handling strategies.

change the trading direction in specific periods. For instance, under the balanced strategy the RVPP becomes a net buyer during 09:15–09:30 in the 15-minute market, while the hourly model does not reflect this change.

Table 5 compares the normalized absolute differences between the hourly and 15-minute schedules of RVPP traded energy in the DAM and traded up/down reserve in the SRM, for different uncertainty-handling strategies. For each hour, the hourly schedule is mapped to its four corresponding 15-minute periods; absolute deviations are computed period by period, summed over the full horizon, and then normalized by the total traded quantity in the hourly schedule. Larger percentages indicate stronger intra-hour variability captured by the 15-minute formulation but smoothed in the hourly formulation. In the deterministic strategy, this leads to normalized differences of 18.0%, 64.4%, and 15.6% for traded energy, up reserve, and down reserve, respectively. When uncertainty is considered (optimistic, balanced, and pessimistic strategies), the normalized differences do not increase monotonically; however, a generally increasing tendency is observed toward more conservative settings. For instance, under the pessimistic strategy the normalized differences reach their maximum values of 34.2%, 65.6%, and 16.3%. A key reason is that in more conservative strategies the RVPP typically trades less energy and reserve, so a given absolute mismatch between 15-minute and hourly schedules translates into a larger normalized deviation.

4.5. Case 3

Fig. 8 compares the DAM price and the up/down SRM prices obtained with the proposed MBRO framework and the *classic*, single-bound RO model (referred to as SB in the results depicted below) under different uncertainty-handling strategies, considering a 15-minute market resolution. Overall, the RO formulation produces more frequent and abrupt

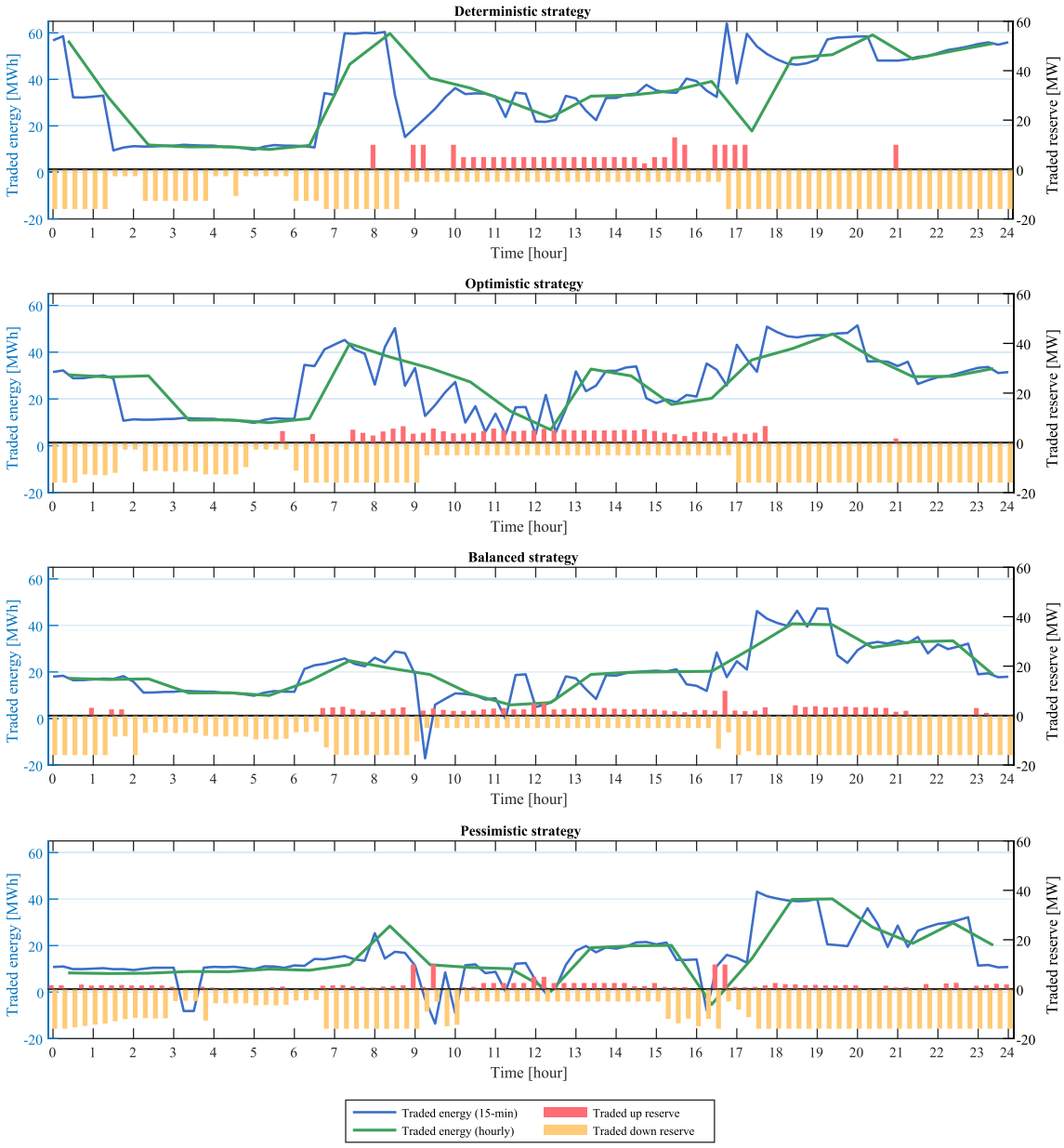


Fig. 7. Case 2 – Total traded energy and reserve of the RVPP in hourly and 15-minute intervals for different uncertainty-handling strategies.

Table 5
Normalized absolute differences (%) between hourly and 15-minute traded energy in the DAM and up/down reserve in the SRM, for different uncertainty-handling strategies.

Strategy	Energy [%]	Up reserve [%]	Down reserve [%]
Deterministic	18.0	64.4	15.6
Optimistic	20.7	28.7	10.1
Balanced	18.7	59.5	11.1
Pessimistic	34.2	65.6	16.3

deviations in both DAM and SRM prices. For instance, under the optimistic strategy, the DAM price in period 1:45–2:00 deviates downward by about 70% relative to the median value. Similar sharp negative DAM deviations appear in other periods, such as 17:45–20:00, 20:45–21:00, 22:30–23:00, and 23:15–23:30. In contrast, under the proposed MBRO framework, price deviations are distributed across multiple bounds, so moderate deviations occur more often while extreme deviations are less frequent, yielding a less conservative and more realistic representation of market prices. For example, in the optimistic strategy, the MBRO model allows low deviations in 16 periods, medium deviations in 4 periods, and high deviations in only 2 periods (see Table 3). As the bidding strategy becomes more conservative (balanced and pessimistic), price deviations occur in more periods in both formulations. Nevertheless, a clear difference remains: the single-bound RO model tends to push prices to their worst-case values more often, resulting in very conservative trajectories with abrupt jumps, whereas the MBRO model yields smoother behavior, with frequent low deviations and relatively rare extreme deviations.

Fig. 9 compares the energy generation and consumption of the uncertainty-affected RVPP units obtained with the proposed MBRO framework and the classic RO model under different uncertainty-handling strategies. In the RO model, uncertainty is represented through a single worst-case realization, which translates into only acute

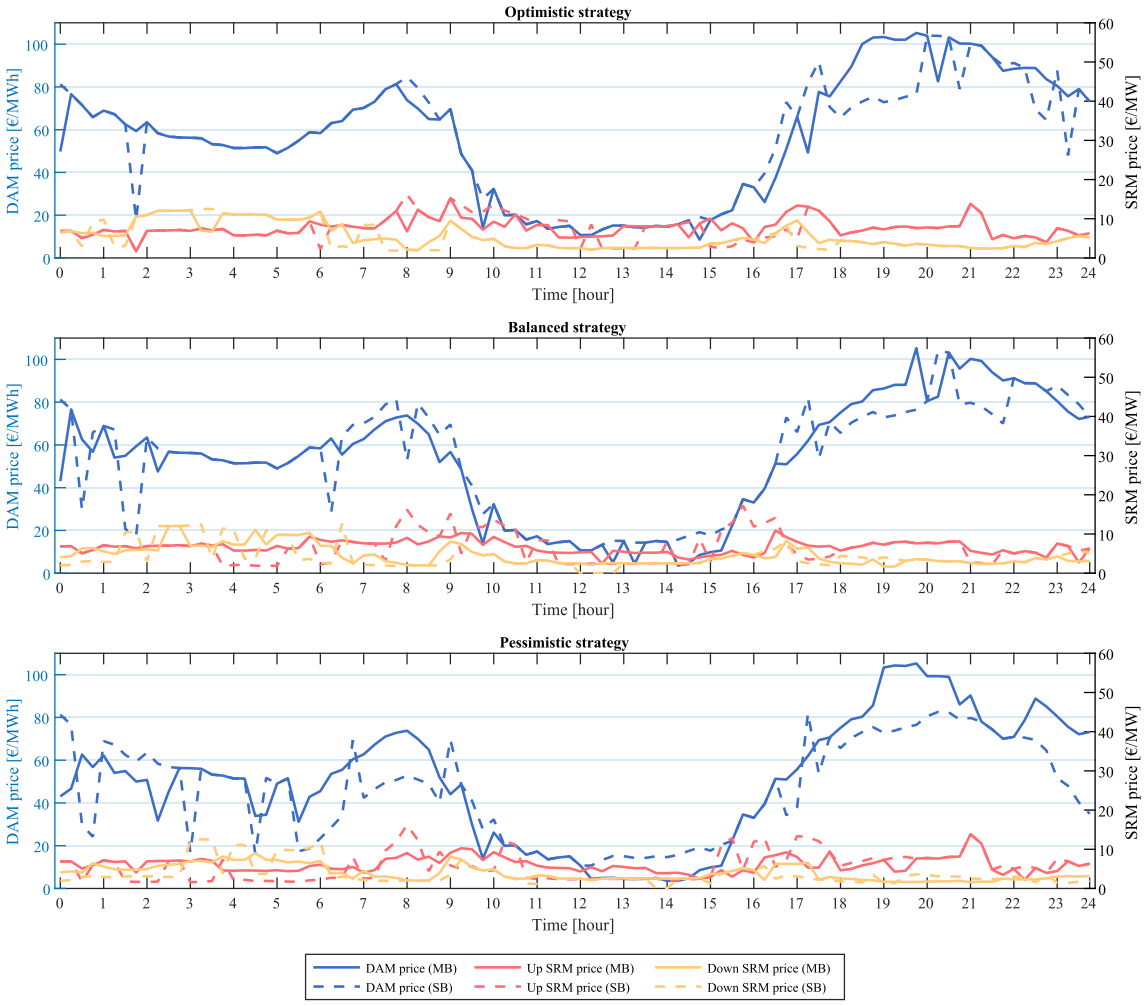


Fig. 8. Case 3 – Electricity price in multi-bound (MB) and single-bound (SB) for different uncertainty-handling strategies.

decreases in wind farm and solar PV production and steep increases in demand consumption. For example, under the optimistic strategy, the wind farm output exhibits negative deviations in periods 0:15–0:45, 8:00–8:15, and 20:15–23:15, with deviations ranging from 55.9% to 59.1% relative to the upper forecast bound. In contrast, the proposed MBRO framework spreads deviations across multiple bounds, so low deviations occur more frequently and very sharp deviations occur less often. When moving from the optimistic to the balanced and pessimistic strategies, the RO model becomes increasingly conservative, driving uncertain generation/consumption close to their worst-case levels in most periods. By comparison, the proposed MBRO approach remains less conservative, with uncertainty primarily reflected through low and medium deviations and with extreme deviations appearing in relatively few periods.

Fig. 10 compares the traded energy of the RVPP obtained with the proposed MBRO framework and the classic RO model under different uncertainty-handling strategies. The traded reserve of the RVPP under the proposed MBRO framework is also shown in the figure. The traded reserve of the RVPP under the RO model, which was previously reported in Fig. 7, is omitted here to avoid cluttering the figure. Overall, the RO approach leads to a much more conservative trading strategy for the RVPP in both the DAM and the SRM compared to the MBRO approach, confirming the observations discussed above.

Table 6 compares the economic results of RVPP participation in the DAM and SRM, obtained using the proposed MBRO framework and the classic RO model under different uncertainty-handling strategies. The table reports the revenue from trading energy and reserve, the operation cost of RVPP units, the robust cost (i.e., the third line in the objective function (12a)), and the resulting profit, defined as revenue minus the operation and robust costs. It also reports the computational time of the simulations. Overall, the MBRO model returns higher profit and lower robust cost than the RO model across all uncertainty-handling strategies. To compare the profit differences on a common scale while avoiding inflated ratios when the corresponding RO profit is small, let $\mathcal{P}^{MB}_{\ell}$ and $\mathcal{P}^{SB}_{\ell}$ denote the profits obtained under strategy ℓ using the multi-bound and single-bound models, respectively. The normalized profit gain and the conventional relative profit gain are defined as $\mathrm{NPG}_{\ell} \triangleq 100\,\frac{\mathcal{P}^{MB}_{\ell}-\mathcal{P}^{SB}_{\ell}}{\mathcal{P}^{SB}_{\mathrm{Opt}}}$ and $\mathrm{RPG}_{\ell} \triangleq 100\,\frac{\mathcal{P}^{MB}_{\ell}-\mathcal{P}^{SB}_{\ell}}{\mathcal{P}^{SB}_{\ell}}$, respectively, where $\mathcal{P}^{SB}_{\mathrm{Opt}}$ is the optimistic single-bound profit used as a common denominator across the three strategies. The resulting NPG_{ℓ} values are approximately 24.9%, 42.8%, and 49.2% under the optimistic, balanced, and pessimistic strategies, respectively. These values represent normalized profit differences rather than conventional strategy-by-strategy percentage improvements. The corresponding RPG_{ℓ} values are approximately 24.9%, 90.9%, and 398.7%, respectively. The large value obtained under the pessimistic strategy results from the small corresponding RO profit and should therefore be interpreted together with the absolute profit values reported in Table 6.

Moreover, the robust cost of the MBRO model is lower than that of the RO model; under the optimistic, balanced, and pessimistic strategies, the corresponding reductions are 26.7%, 19.3%, and 8.5%, respectively.

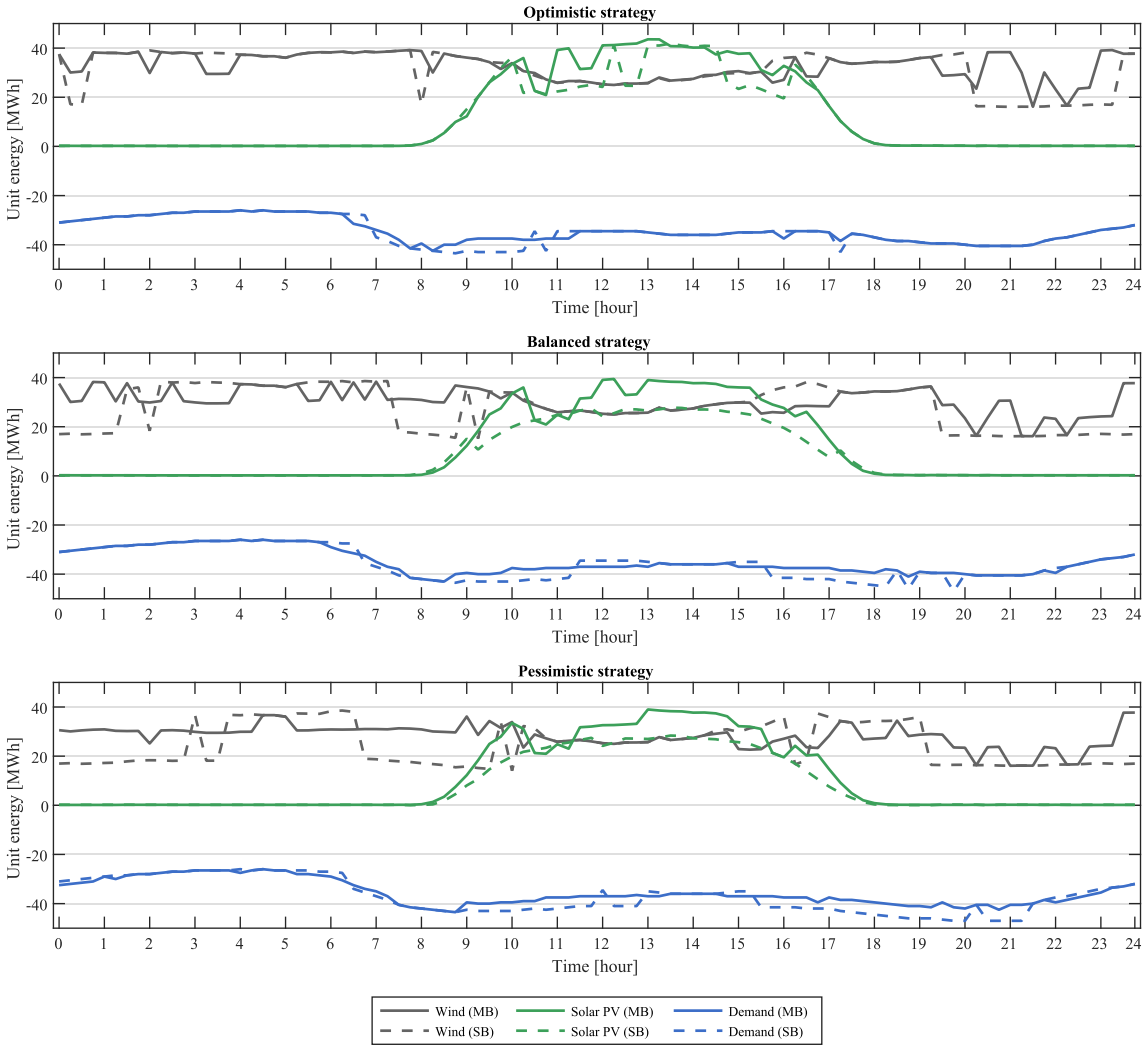


Fig. 9. Case 3 – Unit energy in multi-bound and single-bound for different uncertainty-handling strategies.

Finally, within the RO model, adopting the more conservative balanced and pessimistic strategies (relative to the optimistic strategy) reduces the RVPP profit by 52.9% and 87.6%, respectively. In contrast, the corresponding profit reductions in the MBRO approach are more moderate, at 28.0% and 50.7%. Regarding the computational time, the RO approach typically solves in less than 10 s for all uncertainty-handling strategies. The proposed MBRO approach requires higher computational effort, but for the considered RVPP it is usually solved in less than 1 minute across the different strategies. This comparison indicates that, while the MBRO approach provides greater flexibility for RVPP operators to handle multiple sources of uncertainty, its computational burden remains moderate and does not increase excessively compared to the simpler RO approach. Therefore, the proposed MBRO framework is suitable for performing multiple analyses before submitting the final RVPP bid to the market. Overall, these results demonstrate that the proposed approach reduces the excessive conservatism of the classic RO model while retaining practical computational tractability.

Fig. 11 and Table 7 compare the single-bound RO, proposed MBRO, and Wasserstein-DRO approaches using the spring-season dataset. These results complement the November 2025 case study and provide an additional validation period to examine whether the main qualitative findings remain consistent under different seasonal conditions. The three uncertainty-handling frameworks lead to distinct bidding behaviors. The single-bound RO model tends to produce more conservative decisions because the protected deviations are represented through a single uncertainty interval. The Wasserstein-DRO benchmark incorporates distributional ambiguity through an empirical scenario distribution and market-specific Wasserstein radii, which lead to a different pattern of adjustment in traded energy and reserve. In contrast, the proposed MBRO approach distinguishes frequent moderate deviations from rare extreme deviations through multiple uncertainty bounds, enabling the RVPP to distribute its bid adjustments more evenly across time periods.

As shown in Fig. 11, this structure allows the MBRO model to capture intra-hourly uncertainty exposure without forcing the bidding strategy toward the highly conservative behavior of the single-bound RO model. It also prevents the traded-energy adjustments from being concentrated in large changes during only a few specific periods, as may occur in the DRO solution for some strategies and hours. Therefore, the spring-season results confirm that the proposed MBRO framework preserves the balanced bidding behavior observed in the November 2025 case. In addition, Table 7 shows that the impact of the uncertainty-handling strategy remains evident in the spring dataset: moving from optimistic to pessimistic strategies reduces the traded opportunity and profit, while increasing the weight of uncertainty-related cost components. These observations indicate that the proposed framework is not tied to a single month and can adapt to different seasonal renewable-generation, demand, and market-price conditions.

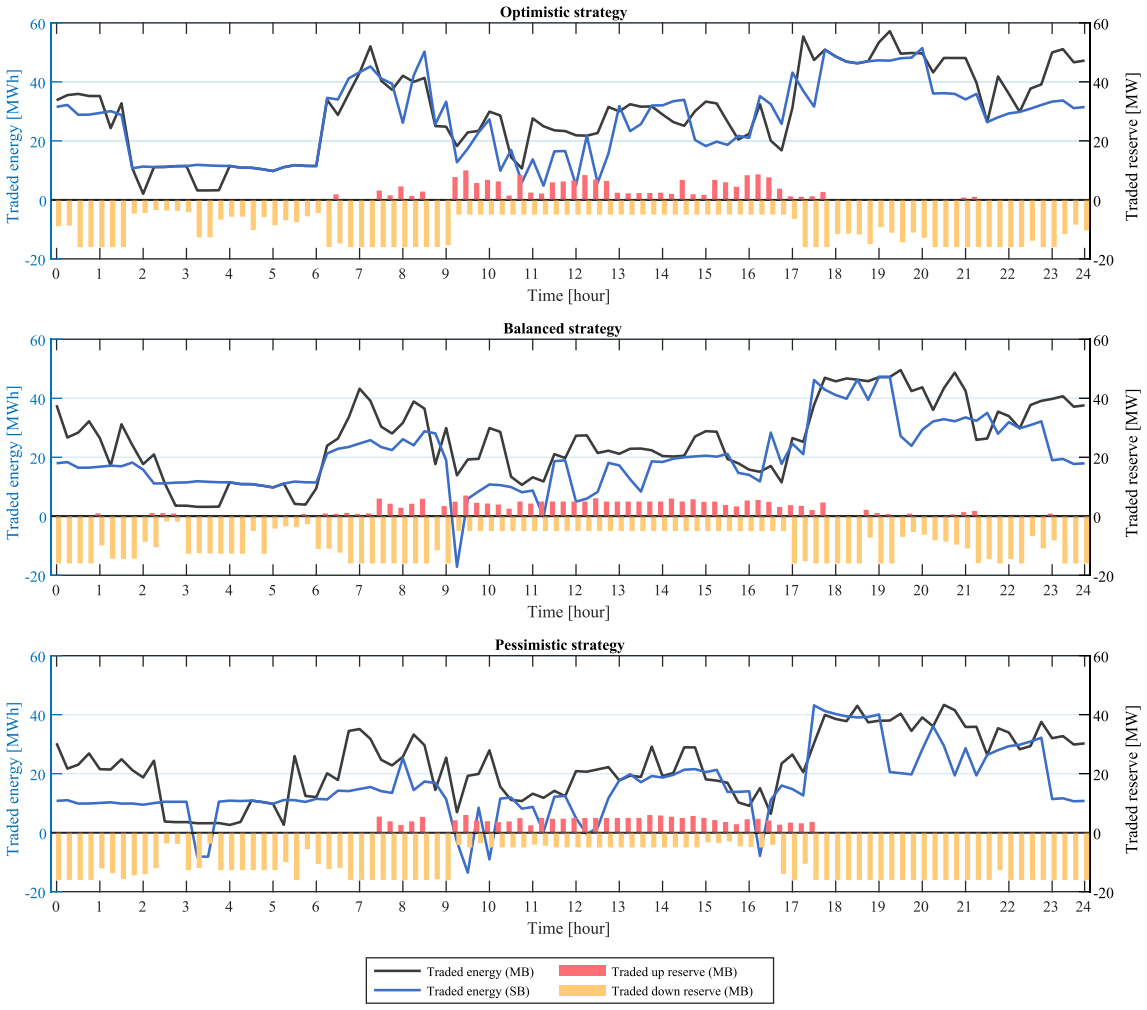


Fig. 10. Case 3 – Total traded energy and reserve of the RVPP in multi-bound and single-bound approaches for different uncertainty-handling strategies.

Table 6
RVPP economic results in multi-bound and single-bound for different uncertainty-handling strategies.

Model	Strategy	Profit [k€]	Revenue [k€]	Operation cost [k€]	Robust cost [k€]	Computational time [s]
SB approach	Optimistic	19.85	46.71	20.98	5.88	3.0
	Balanced	9.35	36.37	19.22	7.80	6.5
	Pessimistic	2.45	28.55	17.76	8.34	4.7
MB approach	Optimistic	24.81	51.01	21.89	4.31	59.5
	Balanced	17.85	44.87	20.73	6.29	38.8
	Pessimistic	12.22	39.78	19.93	7.63	17.9

The computational results in Table 7 also show that the proposed MBRO approach remains more computationally efficient than the Wasserstein-DRO benchmark for all uncertainty-handling strategies. Finally, since the values in Table 7 correspond to bidding-stage optimization outputs before the market uncertainty is realized, the realized performance of the obtained bidding decisions is further evaluated in Section 4.7. This additional out-of-sample assessment provides the final comparison of the single-bound RO, proposed MBRO, and Wasserstein-DRO approaches under realized uncertainty scenarios.

To further assess the computational practicality of the proposed approach, Table 8 reports the profit and computational time obtained for two RVPP sizes, namely a 5-unit case and an enlarged 23-unit case, with the optimality gap set to zero. In the 5-unit case, the model includes 17,410 equations, 13,182 continuous variables, and 3745 binary variables. For the 23-unit case, these values increase to 62,788 equations, 46,454 continuous variables, and 13,350 binary variables, respectively. Despite this substantial increase in model size, the proposed formulation remains computationally tractable. The maximum computational time is 93.2 s for the 5-unit RVPP and 368.2 s for the 23-unit RVPP, corresponding to approximately 1.6 min and 6.1 min, respectively. The solution time differs across the uncertainty-handling strategies and does not follow a strictly monotonic trend. This behavior is expected because different uncertainty-budget settings require the optimization model to explore different combinations of uncertain-parameter realizations when identifying the worst-case exposure. Therefore, the computational burden depends not only on the number of units, but also on

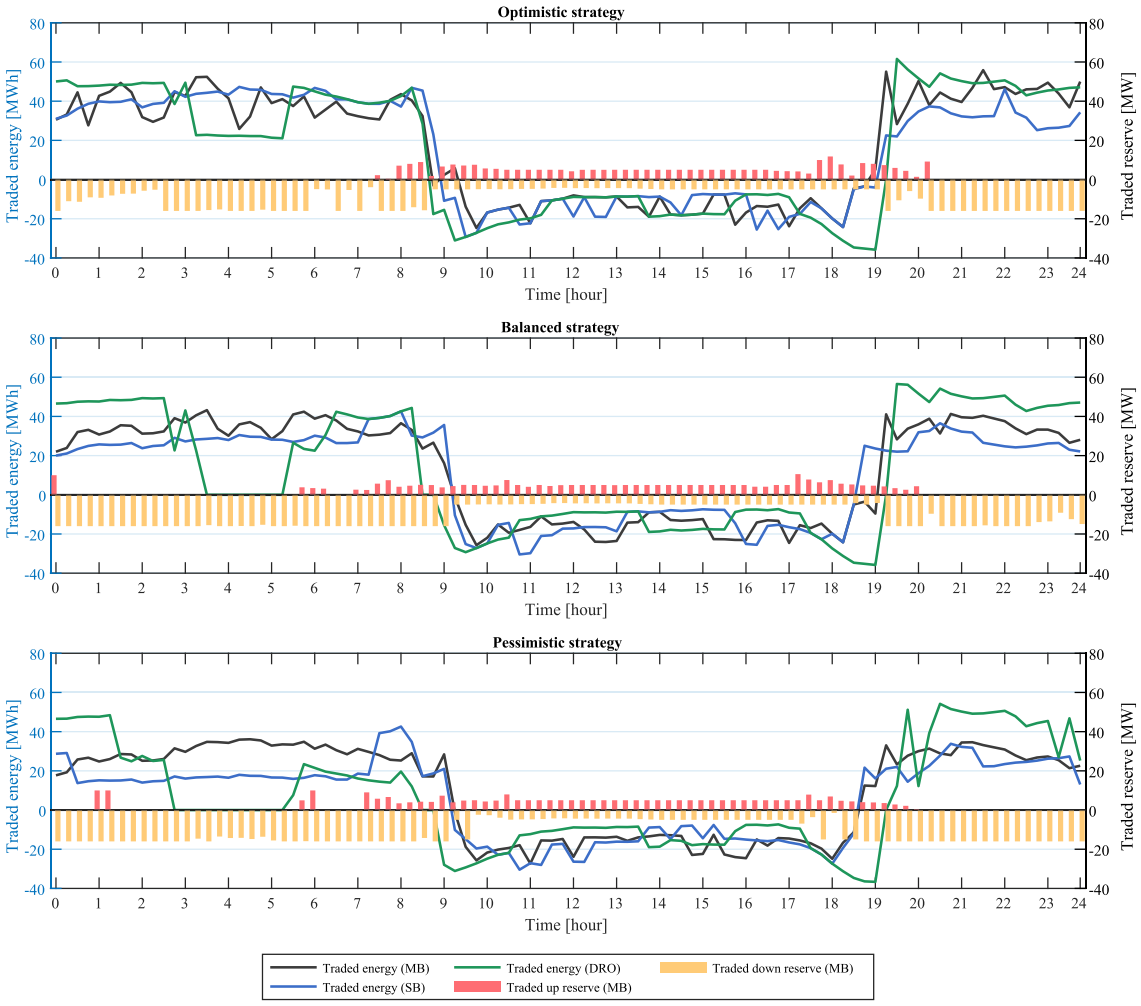


Fig. 11. Case 3 – Total traded energy and reserve of the RVPP in single-bound, multi-bound, and DRO approaches for different uncertainty-handling strategies (spring-season data).

Table 7
RVPP economic results in single-bound, multi-bound, and DRO for different uncertainty-handling strategies (spring-season data).

Model	Strategy	Profit [k€]	Revenue [k€]	Operation cost [k€]	Robust cost/ Wasserstein cost [k€]	Computational time [s]
SB approach	Optimistic	10.95	36.67	18.05	7.67	0.8
	Balanced	2.23	29.44	16.34	10.87	0.3
	Pessimistic	−3.50	23.63	14.81	12.32	0.3
MB approach	Optimistic	15.64	40.29	18.50	6.15	21.3
	Balanced	7.85	34.44	17.45	9.13	30.4
	Pessimistic	2.25	29.68	16.74	10.70	93.2
DRO approach	Optimistic	26.72	48.09	19.70	1.67	550.3
	Balanced	15.05	37.14	17.82	4.27	353.8
	Pessimistic	6.57	26.98	15.77	4.64	479.7

the active uncertainty structure and the resulting branch-and-bound search. Overall, the obtained solution times remain within a practical time scale for DAM bidding studies. This is particularly important in practical applications, where the RVPP operator may need to perform several sensitivity analyses before submitting the final market bid. Hence, the proposed methodology can provide detailed sensitivity information, as illustrated in Section 4.6, while preserving the computational efficiency required for practical RVPP scheduling and bidding applications.

Table 8
Profit and computational time of the MBRO approach for RVPPs with 5 and 23 units under different uncertainty-handling strategies (spring-season data).

Strategy	Profit [k€]		Computational time [s]	
	5-unit	23-unit	5-unit	23-unit
Optimistic	15.64	46.73	21.3	368.2
Balanced	7.85	20.02	30.4	79.9
Pessimistic	2.25	2.72	93.2	142.1

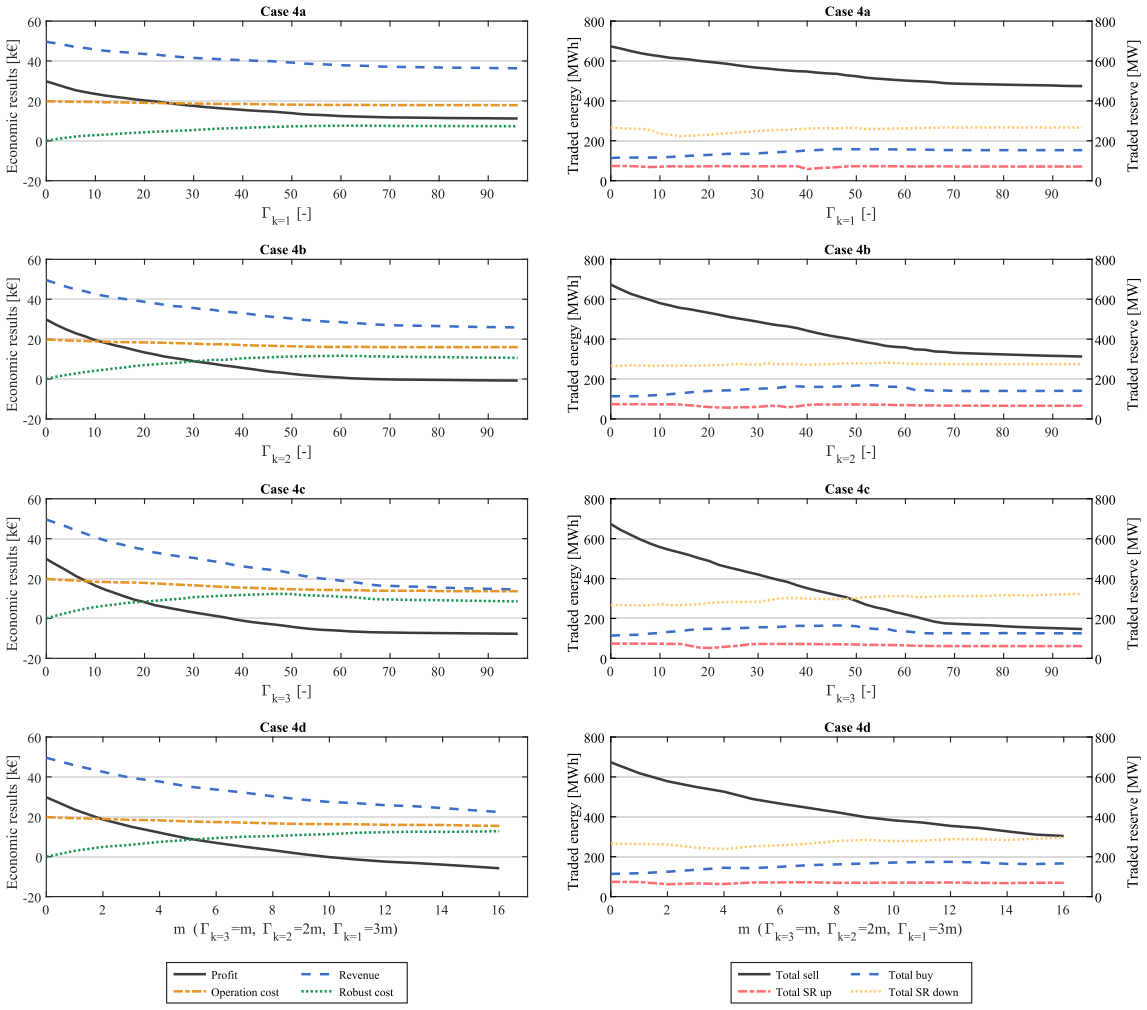


Fig. 12. Case 4 – Sensitivity analysis of economic results and trading decisions for the RVPP under different uncertainty-budget settings: Case 4a varies only $\Gamma_{k=1}$, Case 4b varies only $\Gamma_{k=2}$, Case 4c varies only $\Gamma_{k=3}$, and Case 4d varies all budgets according to $(\Gamma_{k=1}, \Gamma_{k=2}, \Gamma_{k=3}) = (3\text{ m}, 2\text{ m}, \text{m})$.

4.6. Case 4

Fig. 12 presents the sensitivity analysis of the uncertainty budgets used in the proposed MBRO framework. Four budget-setting cases are considered. In Case 4a, only the inner-bound budget $\Gamma_{k=1}$ is increased, while the budgets of the other bounds are fixed at zero. In Case 4b, only the intermediate-bound budget $\Gamma_{k=2}$ is increased. In Case 4c, only the outer-bound budget $\Gamma_{k=3}$ is increased. Finally, in Case 4d, all budgets are increased simultaneously according to $(\Gamma_{k=1}, \Gamma_{k=2}, \Gamma_{k=3}) = (3\text{ m}, 2\text{ m}, \text{m})$.

The results show that the impact of the uncertainty budget depends strongly on the activated bound. In Case 4a, increasing $\Gamma_{k=1}$ from 0 to 96 reduces the RVPP profit from 29.79k€ to 11.18k€ and decreases the total sold energy by 29.6%, while the reserve quantities change only slightly. This indicates that the inner bound mainly represents frequent moderate deviations and therefore leads to a relatively moderate change in the bidding strategy. In Case 4b, the effect becomes stronger: increasing $\Gamma_{k=2}$ from 0 to 96 decreases the total sold energy by 53.5% and reduces the profit to -0.77k€. The most conservative results are obtained in Case 4c, where only $\Gamma_{k=3}$ is varied. Since this bound represents the most severe deviations, increasing $\Gamma_{k=3}$ from 0 to 96 reduces the profit to -7.67k€ and decreases the total sold energy by 78.2%. The upward reserve also decreases by 17.0%, whereas the downward reserve increases by 21.1%.

Case 4d illustrates the benefit of the multi-bound structure. When all uncertainty budgets are increased jointly, the RVPP still becomes more conservative, but the resulting bidding response is more balanced than in the single-bound experiments. At the highest tested combined budget, the total sold energy decreases by 54.8%, which is considerably less severe than the 78.2% reduction observed in Case 4c. Therefore, the proposed MBRO framework allows the RVPP operator to account for frequent moderate deviations and rare extreme deviations simultaneously, avoiding the overly pessimistic decisions that arise when only the most severe bound is activated.

4.7. Case 5

To evaluate the implementability of the obtained bidding decisions, an out-of-sample assessment according to [46] is performed for the single-bound RO, proposed MBRO, and DRO approaches. For the out-of-sample assessment, quarter-hourly historical data are obtained from the Spanish ESIOS platform [44]. The dataset is divided into two non-overlapping and consecutive subsets. Data from 21 February to 23 May 2026, corresponding to 92 complete days, are used exclusively for constructing and calibrating the uncertainty sets and benchmark models. The subsequent 30 complete days, from 24 May to 22 June 2026, are reserved exclusively for the out-of-sample assessment. Thus, the out-of-sample assessment data are fully separated from the model-development data. Each out-of-sample realization corresponds to one complete historical day comprising 96 consecutive 15-minute periods. No synthetic scenario generation, bootstrapping, or

Table 9
Out-of-sample assessment of the single-bound, multi-bound, and DRO approaches under different uncertainty-handling strategies.

Model	Strategy	Average sampled profit [k€]	Average sampled imbalance cost [k€]	Average sampled realized profit [k€]
SB approach	Optimistic	21.77	6.23	15.54
	Balanced	15.74	2.56	13.18
	Pessimistic	10.72	1.08	9.64
MB approach	Optimistic	24.95	8.60	16.35
	Balanced	19.97	4.83	15.14
	Pessimistic	15.92	2.66	13.27
DRO approach	Optimistic	24.10	9.83	14.27
	Balanced	22.72	7.53	15.19
	Pessimistic	14.92	4.38	10.54

random sampling is applied. The DAM, SRM, and imbalance prices, wind and solar PV generation, and demand are aligned using their original historical timestamps. Therefore, the intra-day temporal dependence and the observed cross-variable dependence among the uncertain quantities are preserved. For each model and uncertainty-handling strategy, the optimal bidding decisions are fixed and then tested under the same set of 30 held-out daily realizations of the uncertain parameters. Specifically, the fixed bidding decisions comprise the DAM energy bid and the upward and downward SRM reserve bids, whereas the unit-level operating decisions are optimized separately for each realization. The imbalance settlement uses the upward and downward imbalance prices reported by ESIOS. Surplus energy associated with a positive deviation is sold at the downward imbalance price, while the energy shortage associated with a negative deviation is purchased at the upward imbalance price. This back-testing procedure allows the realized economic performance of the different methods to be compared under identical uncertainty conditions. Three indicators are reported in Table 9: the average sampled profit before imbalance settlement, the average sampled imbalance cost, and the average sampled realized profit after imbalance settlement. The complete out-of-sample formulation, including the imbalance-settlement representation and the definitions of these indicators, is provided in Appendix C.

The results show that the single-bound RO approach achieves the lowest imbalance cost, but this comes at the expense of a more conservative bidding strategy and lower realized profit. In contrast, the proposed MBRO approach provides a more balanced profit–imbalance trade-off. Compared with the single-bound RO approach, the proposed MBRO increases the average realized profit by approximately 5.2%, 14.9%, and 37.7% under the optimistic, balanced, and pessimistic strategies, respectively. Therefore, the proposed approach improves the realized economic performance of the RVPP under out-of-sample uncertainty realizations. Compared with the DRO approach, the proposed MBRO approach also achieves lower imbalance costs in all three strategies. Specifically, the imbalance cost is reduced by approximately 12.5%, 35.9%, and 39.3% in the optimistic, balanced, and pessimistic strategies, respectively. Moreover, MBRO achieves higher realized profit than DRO in the optimistic and pessimistic strategies, while the two approaches provide almost identical realized profit in the balanced strategy. These results confirm that the proposed MBRO framework not only reduces conservatism in the robust optimization formulation but also leads to effective and implementable bidding decisions when evaluated under realized uncertainty.

5. Conclusion

This paper proposes an MBRO framework for the optimal bidding of RVPP in energy and reserve markets, designed to align with the ongoing shift toward higher temporal market resolution (e.g., quarter-hourly scheduling). By deriving an MILP reformulation of the problem, the proposed method provides a mechanism to manage multiple uncertainties, including electricity prices, ND-RES production, and demand, with greater flexibility than classic approaches. Unlike standard RO, the MBRO framework allows for granular control over intra-hourly uncertainty exposure, ensuring protection across a wider range of time intervals without resorting to overly conservative worst-case assumptions. Three main remarks can be drawn from the results of the case studies presented and discussed. First, operational analysis demonstrates that D-RES effectively compensates for renewable fluctuations, while ESS and hydro units anchor the provision of ancillary services. Under uncertainty, the RVPP strategy shifts toward distributing reserve commitments across more intervals with lower individual magnitudes. Second, the comparison of market resolutions highlights the critical importance of granularity; the 15-minute model captures trading dynamics and flow reversals smoothed out by hourly frameworks, with volume discrepancies ranging from 18.0–34.2% for day-ahead energy, 28.7–65.6% for upward reserve, and 10.1–16.3% for downward reserve, based on the scenarios considered. Third, the proposed MBRO approach provides a balanced robust bidding behavior compared with classic RO and a Wasserstein-DRO benchmark by distinguishing between frequent moderate deviations and rare *extreme* deviations. The sensitivity and out-of-sample analyses further show that the selected uncertainty budgets affect the final bidding strategy and that the obtained MBRO schedules remain implementable under realized uncertainty scenarios. Overall, this strategic flexibility improves profitability across different uncertainty-handling strategies while maintaining computational tractability for practical day-ahead bidding studies, including the enlarged RVPP case.

Future work will extend this framework to explicitly model the correlations and non-linear interactions between different uncertainty parameters, further refining the representation of real-world market dynamics.

CRediT authorship contribution statement

Hadi Nemati: Writing – review & editing, Writing – original draft, Visualization, Validation, Software, Resources, Methodology, Investigation, Formal analysis, Data curation, Conceptualization. **Álvaro Ortega:** Writing – review & editing, Validation, Supervision. **Enrique Lobato:** Writing – review & editing, Funding acquisition. **Luis Rouco:** Writing – review & editing, Funding acquisition.

Declaration of competing interest

The authors declare that they have no known competing financial interests or personal relationships that could have appeared to influence the work reported in this paper.

Appendix A. Linear reformulation of the protection functions

To reformulate the protection function of the objective function in (8) as a linear optimization problem (10), we utilize the following proposition based on [38].

Proposition 1. *The value of the protection function in the third line of (8) is equivalent to the optimal objective value of the linear optimization problem (10).*

Proof. The linear maximization problem defined in (10) maximizes its objective by setting the auxiliary variables corresponding to the largest coefficients to 1, contingent on constraint feasibility. Specifically, the optimal solution assigns exactly Γ_k^{DA} of the $z_{k,t}^{DA}$ variables to 1 for each bound k, provided that the limitation on the summation of the auxiliary variables $z_{k,t}^{DA}$ across all uncertainty bounds for any given time period in (10e) is satisfied. Analogous logic applies to the reserve variables, where $\Gamma_k^{SR,\uparrow}$ of the $z_{k,t}^{SR,\uparrow}$ variables and $\Gamma_k^{SR,\downarrow}$ of the $z_{k,t}^{SR,\downarrow}$ variables are set to 1, subject to similar summation limits in constraints (10f) and (10g), respectively. This mechanism is mathematically equivalent to the selection of the worst-case time sets $\left\{\mathcal{T}_k^{DA} \middle| \left|\mathcal{T}_k^{DA}\right| = \Gamma_k^{DA}\right\}$,

$\left\{\mathcal{T}_k^{SR,\uparrow} \middle| \left|\mathcal{T}_k^{SR,\uparrow}\right| = \Gamma_k^{SR,\uparrow}\right\}$, and $\left\{\mathcal{T}_k^{SR,\downarrow} \middle| \left|\mathcal{T}_k^{SR,\downarrow}\right| = \Gamma_k^{SR,\downarrow}\right\}$ utilized in the protection function in (8). □

Additionally, to reformulate the protection function of the ND-RES constraint in (9b) as a linear optimization problem (11), we utilize the following proposition.

Proposition 2. *The value of the protection function on the right-hand side of (9b) is equivalent to the optimal objective value of the linear optimization problem (11).*

Proof. The linear maximization problem defined in (11) maximizes the deviation for the current period $t' = t$ by setting the auxiliary variable $z_{r,k,(t'=t)}$ to 1, contingent on constraint feasibility. Specifically, the optimal solution assigns $z_{r,k,(t'=t)} = 1$ for a chosen bound k if and only if the remaining uncertainty budget (calculated as $\Gamma_{r,k} - \sum_{t' \neq t} z^*_{r,k,t'}$) is sufficient, provided that the limitation on the summation of the auxiliary variable $z_{r,k,(t'=t)}$ across all uncertainty bounds in (11c) is satisfied. This mechanism is mathematically equivalent to determining whether period t can be included in the worst-case time set $\mathcal{T}_{r,k}$ for a specific bound k utilized in the protection function in (9b). □

Appendix B. Wasserstein-DRO benchmark formulation

The Wasserstein-DRO benchmark used for comparison with the proposed model is formulated as follows. The Wasserstein ambiguity sets are defined for the three market-price trajectories. Uncertainty in ND-RES production and demand is represented directly through the historical scenarios and enters the formulation through the scenario-dependent imbalance equation rather than through separate Wasserstein ambiguity sets. Let $\mathcal{N}$ denote the set of historical scenarios, indexed by n, and let $N_s = |\mathcal{N}|$ denote the number of scenarios. Each scenario contains complete trajectories over the scheduling horizon $\mathcal{T}$ of the DAM price $\lambda_{t,n}^{DA}$, the upward and downward SRM prices $\lambda_{t,n}^{SR,\uparrow}$ and $\lambda_{t,n}^{SR,\downarrow}$, the realized ND-RES production $P_{r,t,n}$, and the realized demand $P_{d,t,n}$. All uncertain quantities within a scenario retain their original temporal alignment. Let π_n denote the fixed weight assigned to scenario n, where $\pi_n \geq 0$ and $\sum_{n\in\mathcal{N}} \pi_n = 1$. The three market-price trajectories under scenario n are denoted by $\lambda_n^{DA} = \{\lambda_{t,n}^{DA}\}_{t\in\mathcal{T}}$, $\lambda_n^{SR,\uparrow} = \{\lambda_{t,n}^{SR,\uparrow}\}_{t\in\mathcal{T}}$, and $\lambda_n^{SR,\downarrow} = \{\lambda_{t,n}^{SR,\downarrow}\}_{t\in\mathcal{T}}$. Let $\mathcal{M}^\lambda = \{\lambda^{DA}, \lambda^{SR,\uparrow}, \lambda^{SR,\downarrow}\}$ denote the set of market-price trajectories, with m indexing its elements. The corresponding empirical reference distribution is

$$\hat{\mathbb{P}}_{N_s}^m = \sum_{n\in\mathcal{N}} \pi_n \delta_{\lambda_n^m}\ ; \qquad \forall \lambda^m \in \mathcal{M}^\lambda, \tag{B.1}$$

where $\delta_{\lambda_n^m}$ denotes the Dirac probability distribution concentrated at the historical price trajectory λ_n^m. Thus, $\hat{\mathbb{P}}_{N_s}^m$ represents the weighted empirical distribution constructed from the observed price trajectories. Following the data-driven Wasserstein-DRO framework in [45], a separate first-order Wasserstein ambiguity set is defined for each market-price trajectory as

$$\mathbb{B}^m(\epsilon^m) = \left\{\mathbb{Q}^m : W_1\left(\mathbb{Q}^m, \hat{\mathbb{P}}_{N_s}^m\right) \leq \epsilon^m\right\}\ ; \qquad \forall \lambda^m \in \mathcal{M}^\lambda, \tag{B.2}$$

where $\mathbb{Q}^m$ is a candidate probability distribution, $W_1(\cdot,\cdot)$ denotes the first-order Wasserstein distance evaluated using the ℓ_∞ ground norm over each complete price trajectory, and ϵ^m is the Wasserstein radius associated with market-price trajectory λ^m. Accordingly, ϵ^{DA}, $\epsilon^{SR,\uparrow}$, and $\epsilon^{SR,\downarrow}$ control the ambiguity considered for the DAM, upward-SRM, and downward-SRM prices, respectively.

The DAM energy bid p_t^{DA}, the upward and downward reserve bids $r_t^{SR,\uparrow}$ and $r_t^{SR,\downarrow}$, and the unit-level dispatch, reserve-allocation, and commitment decisions are here-and-now variables that are common to all scenarios. These variables, together with the scenario-dependent imbalance variables and the auxiliary variables introduced below, are collected in the decision set Ξ^{DRO}. Let $\kappa_{t,n}^+$ and $\kappa_{t,n}^-$ denote the scenario-dependent surplus energy and energy shortage, respectively. The dimensionless parameters ρ^+ and ρ^- denote the imbalance multipliers applied to the realized DAM price for surplus energy and energy shortage, respectively. The nonnegative auxiliary variable q_t^{DA} represents the absolute value of the DAM energy bid, which may be positive or negative. To enforce a unique imbalance direction in each period and scenario, let $b_{t,n}^{imb}$ be a binary variable equal to 1 when surplus energy is allowed and 0 when energy shortage is allowed, and let M^{imb} denote a valid upper bound on the magnitude of the energy imbalance. The Wasserstein-DRO benchmark is formulated in (B.3).

$$\max_{\Xi^{DRO}} \Pi^{DRO} = R^{DRO,rev} - C^{DRO,op} - C^{DRO,W}\ ; \tag{B.3a}$$

$$R^{DRO,rev} = \sum_{n\in\mathcal{N}} \pi_n \sum_{t\in\mathcal{T}} \Big[\lambda_{t,n}^{DA} p_t^{DA} \Delta t + \lambda_{t,n}^{SR,\uparrow} r_t^{SR,\uparrow} + \lambda_{t,n}^{SR,\downarrow} r_t^{SR,\downarrow}$$

$$-\rho^- \lambda_{t,n}^{DA} \kappa_{t,n}^- \Delta t + \rho^+ \lambda_{t,n}^{DA} \kappa_{t,n}^+ \Delta t\Big]\ ; \tag{B.3b}$$

$$C^{DRO,op} = \sum_{t\in\mathcal{T}} \sum_{c\in\mathcal{C}} C_c p_{c,t} \Delta t + \sum_{t\in\mathcal{T}} \sum_{r\in\mathcal{R}} C_r p_{r,t} \Delta t + \sum_{t\in\mathcal{T}} \sum_{s\in\mathcal{S}} C_s p_{s,t} \Delta t\ ; \tag{B.3c}$$

$$C^{DRO,W} = \epsilon^{DA} \sum_{t\in\mathcal{T}} q_t^{DA} \Delta t + \epsilon^{SR,\uparrow} \sum_{t\in\mathcal{T}} r_t^{SR,\uparrow} + \epsilon^{SR,\downarrow} \sum_{t\in\mathcal{T}} r_t^{SR,\downarrow}\ ; \tag{B.3d}$$

$$\kappa_{t,n}^- - \kappa_{t,n}^+ = \sum_{r\in\mathcal{R}} \left(p_{r,t} - P_{r,t,n}\right) + \sum_{d\in\mathcal{D}} \left(P_{d,t,n} - p_{d,t}\right)\ ; \quad \forall t, n \in \mathcal{T}, \mathcal{N} \tag{B.3e}$$

$$0 \leq \kappa_{t,n}^+ \leq M^{imb} b_{t,n}^{imb}\ ; \qquad \forall t, n \in \mathcal{T}, \mathcal{N} \tag{B.3f}$$

$$0 \leq \kappa_{t,n}^- \leq M^{imb}\left(1 - b_{t,n}^{imb}\right)\ ; \qquad \forall t, n \in \mathcal{T}, \mathcal{N} \tag{B.3g}$$

$$b_{t,n}^{imb} \in \{0,1\}\ ; \qquad \forall t, n \in \mathcal{T}, \mathcal{N} \tag{B.3h}$$

$$q_t^{DA} \geq p_t^{DA}\ ; \qquad \forall t \in \mathcal{T} \tag{B.3i}$$

$$q_t^{DA} \geq -p_t^{DA}\ ; \qquad \forall t \in \mathcal{T} \tag{B.3j}$$

Eq. (B.3a) maximizes the DRO objective value Π^{DRO}. The scenario-weighted net market revenue $R^{DRO,rev}$ in (B.3b) includes the DAM and SRM revenues together with the imbalance settlement associated with energy shortage and surplus energy through ρ^- and ρ^+, respectively. Thus, an energy shortage reduces the net market revenue, whereas surplus energy increases it according to the corresponding imbalance multiplier. The operating cost $C^{DRO,op}$ in (B.3c) is calculated from the here-and-now schedules of the D-RES, ND-RES, and ESS units. The Wasserstein cost $C^{DRO,W}$ in (B.3d) is the decision-dependent ambiguity penalty associated with the three market-specific Wasserstein radii and the corresponding energy and reserve bids. It is subtracted from the objective function and is not a physical operating or market payment. Constraint (B.3e) calculates the scenario-dependent energy shortage or surplus caused by deviations of ND-RES production and demand from their here-and-now scheduled values. When realized ND-RES production is lower than its scheduled value or realized demand is higher than its scheduled value, the right-hand side of (B.3e) is positive and is represented by the shortage variable $\kappa_{t,n}^-$; conversely, higher realized ND-RES production or lower realized demand produces surplus energy represented by $\kappa_{t,n}^+$. Constraints (B.3f) and (B.3g), together with the binary-domain constraint (B.3h), enforce mutual exclusivity between surplus and shortage in each period and scenario. Specifically, $b_{t,n}^{imb} = 1$ allows only $\kappa_{t,n}^+$ to be positive, whereas $b_{t,n}^{imb} = 0$ allows only $\kappa_{t,n}^-$ to be positive. Constraints (B.3i) and (B.3j) enforce $q_t^{DA} \geq |p_t^{DA}|$; because q_t^{DA} is penalized in the objective function, equality holds at the optimum. The Wasserstein-DRO problem is also subject to the remaining here-and-now supply–demand, D-RES, ND-RES, demand, ESS, and reserve-provision constraints presented in Section 3.1, which are not repeated here for brevity.

Appendix C. Out-of-sample assessment

The out-of-sample assessment in this paper is performed according to [46]. Let Ω denote the set of out-of-sample realizations, indexed by ω. For each realization $\omega \in \Omega$, the optimal market bids obtained from the evaluated models are fixed. These bids comprise the energy bid p_t^{DA*}

and the upward and downward reserve bids $r_t^{SR,\uparrow^*}$ and $r_t^{SR,\downarrow^*}$, respectively. The unit-level operating variables are then optimized for each realization of the uncertain parameters ($\lambda_{t,\omega}^{DA}$, $\lambda_{t,\omega}^{SR,\uparrow}$, $\lambda_{t,\omega}^{SR,\downarrow}$, $\lambda_{t,\omega}^{imb,\uparrow}$, $\lambda_{t,\omega}^{imb,\downarrow}$, $P_{r,t,\omega}$, and $P_{d,t,\omega}$). These variables, together with the deviation and binary variables introduced below, are collected in the decision set Ξ_ω^{OOS} associated with realization ω. Let $\kappa_{t,\omega}^{+}$ and $\kappa_{t,\omega}^{-}$ denote the positive and negative energy deviations, respectively, between the realized net delivery of the RVPP and its fixed DAM energy bid. A positive deviation represents surplus energy sold at the downward imbalance price $\lambda_{t,\omega}^{imb,\downarrow}$, whereas a negative deviation represents an energy shortage purchased at the upward imbalance price $\lambda_{t,\omega}^{imb,\uparrow}$. Mutual exclusivity between the two deviations is enforced using the binary variable $b_{t,\omega}^{imb}$ and a valid upper bound M^{imb} on the magnitude of the energy imbalance. Additionally, to represent the reserve state vectors consistently with (2), we define the unit reserve vector for realization ω as $\boldsymbol{r}_{u,t,\omega} = \{r_{u,t,\omega}^{\uparrow}, -r_{u,t,\omega}^{\downarrow}, 0\}$ and the fixed market reserve-bid vector as $\boldsymbol{r}_t^{SR,*} = \{r_t^{SR,\uparrow^*}, -r_t^{SR,\downarrow^*}, 0\}$. The out-of-sample problem for realization ω is formulated in (C.1).

$$\max_{\Xi_\omega^{OOS}} \Pi_\omega^{real} = \Pi_\omega^{sam} - C_\omega^{imb} \qquad \forall \omega \in \Omega \tag{C.1a}$$

$$\Pi_\omega^{sam} = \sum_{t\in\mathcal{T}} \left[\lambda_{t,\omega}^{DA} p_t^{DA^*} \Delta t + \lambda_{t,\omega}^{SR,\uparrow} r_t^{SR,\uparrow^*} + \lambda_{t,\omega}^{SR,\downarrow} r_t^{SR,\downarrow^*}\right] - \sum_{t\in\mathcal{T}}\sum_{c\in\mathscr{C}} C_c p_{c,t,\omega}\Delta t - \sum_{t\in\mathcal{T}}\sum_{r\in\mathscr{R}} C_r p_{r,t,\omega}\Delta t - \sum_{t\in\mathcal{T}}\sum_{s\in\mathcal{S}} C_s p_{s,t,\omega}\Delta t \quad \forall \omega \in \Omega \tag{C.1b}$$

$$C_\omega^{imb} = \sum_{t\in\mathcal{T}} \left[\lambda_{t,\omega}^{imb,\uparrow}\kappa_{t,\omega}^{-} - \lambda_{t,\omega}^{imb,\downarrow}\kappa_{t,\omega}^{+}\right]\Delta t \qquad \forall \omega \in \Omega \tag{C.1c}$$

$$\sum_{r\in\mathscr{R}}\left[p_{r,t,\omega} + \boldsymbol{r}_{r,t,\omega}\right] + \sum_{s\in\mathcal{S}}\left[p_{s,t,\omega} + \boldsymbol{r}_{s,t,\omega}\right] + \sum_{c\in\mathscr{C}}\left[p_{c,t,\omega} + \boldsymbol{r}_{c,t,\omega}\right] - \sum_{d\in\mathscr{D}}\left[p_{d,t,\omega} - \boldsymbol{r}_{d,t,\omega}\right] = p_t^{DA^*} + \boldsymbol{r}_t^{SR,*} + \kappa_{t,\omega}^{+} - \kappa_{t,\omega}^{-} \quad \forall t,\omega \in \mathcal{T},\Omega \tag{C.1d}$$

$$0 \le \kappa_{t,\omega}^{+} \le M^{imb} b_{t,\omega}^{imb} \qquad \forall t,\omega \in \mathcal{T},\Omega \tag{C.1e}$$

$$0 \le \kappa_{t,\omega}^{-} \le M^{imb}\left(1 - b_{t,\omega}^{imb}\right) \qquad \forall t,\omega \in \mathcal{T},\Omega \tag{C.1f}$$

$$b_{t,\omega}^{imb} \in \{0,1\} \qquad \forall t,\omega \in \mathcal{T},\Omega \tag{C.1g}$$

Eq. (C.1a) defines the realized-profit objective for each realization ω. In (C.1b), Π_ω^{sam} is the sampled profit before imbalance settlement. The energy revenue is calculated using the fixed energy bid, $p_t^{DA^*}$, and the corresponding realized DAM price $\lambda_{t,\omega}^{DA}$. The reserve revenues are calculated using the fixed reserve bids and the realized upward and downward SRM prices. The operating costs in the second line of (C.1b) are calculated from the dispatch variables $p_{c,t,\omega}$, $p_{r,t,\omega}$, and $p_{s,t,\omega}$ corresponding to realization ω. Eq. (C.1c) calculates the net imbalance cost according to the Spanish settlement mechanism. The energy shortage associated with a negative deviation $\kappa_{t,\omega}^{-}$ is purchased at the upward imbalance price $\lambda_{t,\omega}^{imb,\uparrow}$, which is usually higher than the corresponding DAM price. The surplus energy associated with a positive deviation $\kappa_{t,\omega}^{+}$ is sold at the downward imbalance price $\lambda_{t,\omega}^{imb,\downarrow}$, which is usually lower than the corresponding DAM price. Constraint (C.1d) links the positive and negative deviation variables to the physical power balance for each realization. The market energy and reserve bids on the right-hand side are fixed at the optimal values obtained from the evaluated models, whereas the unit dispatch and reserve-allocation variables on the left-hand side are optimized separately for each realization ω. When the realized net delivery exceeds the fixed market commitment, the surplus is represented by $\kappa_{t,\omega}^{+}$. When the realized net delivery is lower than the fixed commitment, the shortage is represented by $\kappa_{t,\omega}^{-}$. Constraints (C.1e)–(C.1g) enforce mutual exclusivity between surplus and shortage in each period and realization. Accordingly, the three indicators reported in Table 9 are calculated in (C.2).

$$\Pi^{sam,av} = \frac{1}{|\Omega|}\sum_{\omega\in\Omega}\Pi_\omega^{sam}\ ; \tag{C.2a}$$

$$C^{imb,av} = \frac{1}{|\Omega|}\sum_{\omega\in\Omega}C_\omega^{imb}\ ; \tag{C.2b}$$

$$\Pi^{real,av} = \frac{1}{|\Omega|}\sum_{\omega\in\Omega}\Pi_\omega^{real} = \Pi^{sam,av} - C^{imb,av}\ ; \tag{C.2c}$$

The symbols $\Pi^{sam,av}$, $C^{imb,av}$, and $\Pi^{real,av}$ in (C.2a)–(C.2c) correspond to the average sampled profit, average sampled imbalance cost, and average sampled realized profit reported in Table 9, respectively. The out-of-sample problem is subject to the relevant operational constraints presented in Section 3.1, applied separately to each realization ω. These constraints are not repeated here for brevity.

Data availability

Data will be made available on request.

References

[1] Prete CL, Palmer K, Robertson M. Time for a market upgrade? A review of wholesale electricity market designs for the future. Energy Econ 2025;108640.
[2] European Commission. Electricity market design; 2025. https://energy.ec.europa.eu/topics/markets-and-consumers/electricity-market-design_en.
[3] Red Eléctrica de España (REE). 2025. https://www.ree.es/en (Accessed: 11 August 2026).
[4] OMI, Polo Español S.A. (OMIE). OMIE. 2026. https://www.omie.es/en (Accessed: 11 August 2026).
[5] European Network of Transmission System Operators for Electricity (ENTSO-E). Electricity balancing overview and imbalance settlement; 2025. https://www.entsoe.eu/network_codes/eb/.
[6] Yang C, Du X, Xu D, Tang J, Lin X, Xie K, Li W. Optimal bidding strategy of renewable-based virtual power plant in the day-ahead market. Int J Electr Power Energy Syst 2023;144:108557.
[7] Gao H, Jin T, Feng C, Li C, Chen Q, Kang C. Review of virtual power plant operations: resource coordination and multidimensional interaction. Appl Energy 2024;357:122284.
[8] Kaiss M, Wan Y, Gebbran D, Vila CU, Dragičević T. Review on virtual power Plants/Virtual aggregators: concepts, applications, prospects and operation strategies. Renew Sustain Energy Rev 2025;211:115242.
[9] Liu J, Peng J, Liu H, Deng J, Song X. Two-stage robust optimization of a virtual power plant considering a refined demand response. Energy 2025;322:135560.
[10] Wu S, Wang Y, Liu L, Yang Z, Cao Q, He H, Cao Y. Two-stage distributionally robust optimal operation of rural virtual power plants considering multi correlated uncertainties. Int J Electr Power Energy Syst 2024;161:110173.
[11] Feng J, Ran L, Wang Z, Zhang M. Optimal energy scheduling of virtual power plant integrating electric vehicles and energy storage systems under uncertainty. Energy 2024;309:132988.
[12] Li Y, Deng Y, Wang Y, Jiang L, Shahidehpour M. Robust bidding strategy for multi-energy virtual power plant in peak-regulation ancillary service market considering uncertainties. Int J Electr Power Energy Syst 2023;151:109101.
[13] Falabretti D, Gulotta F, Siface D. Scheduling and operation of RES-based virtual power plants with e-mobility: a novel integrated stochastic model. Int J Electr Power Energy Syst 2023;144:108604.
[14] Cao J, Xu C, Siqin Z, Yu M, Diao R. Scenario-driven distributionally robust optimization model for a rural virtual power plant considering flexible energy-carbon-green certificate trading. Appl Energy 2025;379:124904.
[15] Wang Y, Huang W, Chen H, Yu Z, Hu L, Huang Y. Optimal scheduling strategy for virtual power plants with aggregated user-side distributed energy storage and photovoltaics based on CVaR-distributionally robust optimization. J Energy Storage 2024;86:110770.
[16] Mei S, Tan Q, Trivedi A, Srinivasan D. A two-step optimization model for virtual power plant participating in spot market based on energy storage power distribution considering comprehensive forecasting error of renewable energy output. Appl Energy 2024;376:124234.
[17] Xiao D, Lin Z, Chen H, Hua W, Yan J. Windfall profit-aware stochastic scheduling strategy for industrial virtual power plant with integrated risk-seeking/averse preferences. Appl Energy 2024;357:122460.
[18] Shafiekhani M, Ahmadi A, Homaee O, Shafie-Khah M, Catalão JP. Optimal bidding strategy of a renewable-based virtual power plant including wind and solar units and dispatchable loads. Energy 2022;239:122379.
[19] Afzali S, Moghaddam MP, Sheikh-El-Eslami MK, Zamani R. A flexibility-oriented bidding strategy for virtual power plants incorporating local energy communities: a bi-level stochastic-robust methodology. Appl Energy 2025;399:126355.
[20] Ma Y, Li Z, Liu R, Liu B, Yu SS, Liao X, Shi P. Data-driven interval robust optimization method of VPP bidding strategy in spot market under multiple uncertainties. Appl Energy 2025;384:125366.
[21] Wang J, Xu J, Wang J, Ke D, Yao L, Zhou Y, Liao S. Two-stage distributionally robust offering and pricing strategy for a price-maker virtual power plant. Appl Energy 2024;363:123005.

[22] Zhu Y, Wei N, Kang J, Tian Y. Low-carbon and robust economic scheduling of virtual power plants considering multiple uncertainties. Sustain Energy Grids Netw 2025;102104.
[23] Shang Y, Li X, Xu T, Cui L. Uncertainty-output virtual power plant participates in multi-electricity market considering the improved Shapley value distribution method. Int J Electr Power Energy Syst 2025;165:110462.
[24] Feng J, Ran L, Wang Z, Zhang M. Optimal bidding strategy for virtual power plant in multiple markets considering integrated demand response and energy storage. J Energy Storage 2025;124:116706.
[25] Du H, Hu J, Fang Y, Xie D. Optimal bidding strategy for virtual power plant participating in joint energy and reserve market considering physical-economic feasible operation region. Energy 2025;138410.
[26] Siqin Z, Diao R, Zhao M. Two-stage distributionally robust bidding strategies for multi-energy virtual power plants in energy, reserve and carbon markets. Energy 2025;137455.
[27] Esfahani M, Alizadeh A, Cao B, Kamwa I, Xu M. A stochastic-robust aggregation strategy for VPP to participate in the frequency regulation market via backup batteries. J Energy Storage 2024;98:113057.
[28] Nokandi E, Vahedipour-Dahraie M, Goldani SR, Siano P. A three-stage bi-level model for joint energy and reserve scheduling of VPP considering local intraday demand response exchange market. Sustain Energy Grids Netw 2023;33:100964.
[29] Zamani AG, Zakariazadeh A, Jadid S. Day-ahead resource scheduling of a renewable energy based virtual power plant. Appl Energy 2016;169:324–40.
[30] Nemati H, Sánchez-Martín P, Ortega Á, Sigrist L, Lobato E, Rouco L. Flexible robust optimal bidding of renewable virtual power plants in sequential markets under asymmetric uncertainties. Sustain Energy Grids Netw 2025;101801.
[31] Nemati H, Sánchez-Martín P, Baringo A, Ortega Á. Single-level flexible robust optimal bidding of renewable-only virtual Power plant in energy and secondary reserve markets. Energy 2025;136421.
[32] Nemati H, Sánchez-Martín P, Ortega Á, Sigrist L, Rouco L. Integration of concentrated solar power plants in renewable-only VPP with electrical and thermal demands: a two-stage robust bidding approach. J Energy Storage 2026;141:119265.
[33] Li Q, Dong F, Jiang B, Liu J, Yan P, Yu D. Risk-averse co-optimization of virtual power plants in multi-markets considering scheduling costs and uncertainties of controllable loads. Appl Energy 2026;409:127496.
[34] Li W, Dong F, Ji Z, Wang P. Internal and external coordinated distributionally robust bidding strategy of virtual power plant operator participating in day-ahead electricity spot and peaking ancillary services markets. Appl Energy 2025;386:125514.
[35] Yuanyuan Z, Huiru Z, Bingkang L. Distributionally robust comprehensive declaration strategy of virtual power plant participating in the power market considering flexible ramping product and uncertainties. Appl Energy 2023;343:121133.
[36] Wang J, Ilea V, Bovo C, Xie N, Wang Y. Optimal self-scheduling for a multi-energy virtual power plant providing energy and reserve services under a holistic market framework. Energy 2023;278:127903.
[37] Büsing C, D'andreagiovanni F. New results about multi-band uncertainty in robust optimization. In: International symposium on experimental algorithms. Springer; 2012. p. 63–74.
[38] Bertsimas D, Sim M. The price of robustness. Oper Res 2004;52(1):35–53.
[39] Carrión M, Arroyo JM. A computationally efficient mixed-integer linear formulation for the thermal unit commitment problem. IEEE Trans Power Syst 2006;21(3):1371–8.
[40] Zhang Z, Zhou M, Wu Z, Liu S, Guo Z, Li G. A frequency security constrained scheduling approach considering wind farm providing frequency support and reserve. IEEE Trans Sustain Energy 2022;13(2):1086–100.
[41] Yin S, Wang J, Li Z, Fang X. State-of-the-art short-term electricity market operation with solar generation: a review. Renew Sustain Energy Rev 2021;138:110647.
[42] Morales-España G, Lorca Á, de Weerdt MM. Robust unit commitment with dispatchable wind power. Electr Power Syst Res 2018;155:58–66.
[43] Floudas CA. Nonlinear and mixed-integer optimization: fundamentals and applications. Oxford University Press; 1995.
[44] Red Eléctrica. ESIOS: electricidad, datos y transparencia. 2026. https://www.esios.ree.es/ (Accessed: 11 August 2026).
[45] Mohajerin Esfahani P, Kuhn D. Data-driven distributionally robust optimization using the Wasserstein metric: performance guarantees and tractable reformulations. Math Program 2018;171:115–66.
[46] Baringo A, Baringo L, Arroyo JM. Day-ahead self-scheduling of a virtual power plant in energy and reserve electricity markets under uncertainty. IEEE Trans Power Syst 2018;34(3):1881–94.